The Impact of Extreme Low Temperatures on Raman Spectra of Amino Acids Relevant for the Search for Life on Europa

Aria Vitkova[1], Scott J. I. Walker[1], Hanna Sykulska-Lawrence[1]

Abstract

Raman spectroscopy, an emerging technology for *in situ* space exploration, has been suggested for life detection for the Europa Lander Mission. However, obtaining spectra of samples from the Europan icy shell requires measurements at temperatures down to -233 °C, which will affect the Raman spectra of any potential biosignatures. In this study, we obtained Raman spectra of amino acids using a 785 nm Raman system at temperatures ranging down to -196 °C, analogous to Europa's surface and near sub-surface. Significant Raman band width narrowing and decreasing variance were observed at lower temperatures leading to higher precision Raman measurements, which required higher spectral resolution that could be as high as 2 cm^{-1} for full identification of amino acids. Such spectral resolution is much higher than the resolution of contemporary

[1] Astronautics Research Group, University of Southampton, Southampton, SO17 1BJ, UK (phone: +44(0)2380 592313; e-mail: H.M.Sykulska-Lawrence@soton.ac.uk, office: B176/2033)

Raman instruments for planetary exploration and may be particularly problematic for miniaturized instruments. Shifting of Raman bands to both higher and lower frequencies by as much as ~25 cm^{-1} together with changes in the Raman band intensity were recorded. The emergence of new bands and diminishing of the original bands also occurred for some amino acids. A significantly increased fluorescence background was observed in spectra of fluorescent molecules (*i.e.*, Tryptophan). A link between the type of vibrational modes associated with Raman bands and the change in their Raman shift at extreme low temperatures was identified and described. This link offers an exciting new method of molecule identification solely based on the comparison of spectra collected at two different temperatures and could greatly improve the identification capabilities in Raman spectroscopy for a wide array of applications.

Keywords: Astrobiology – Biosignatures – Europa – Extreme Low Temperatures – Life Detection – Raman Spectroscopy

1. Introduction

Jupiter's Moon Europa has been one of the major focus points for astrobiology in recent years due to its high potential for harbouring life in its vast saline ocean underneath its icy crust. The Europan ocean is believed to be in contact with a rocky silicate seafloor, not unlike the seafloor on Earth, which could potentially provide an ideal chemistry balance for the emergence of life (Hand et al., 2017; Zolotov et al., 2004).

However, located in Jupiter's distant high radiation belt, Europa represents a very challenging target for space exploration. Only a limited number of missions have ventured to collect data about this distant ocean world to date. Nevertheless, data collected during these missions suggesting the presence of a liquid saline ocean placed Europa on a high priority list for space exploration and there are now further missions underway to explore Europa and its surface (Anderson et al., 1997; Chyba & Phillips, 2001; Committee on the Planetary Science Decadal Survey, 2011; Hiscox, 2000).

An orbiter mission JUICE, developed by ESA and planned for launch in 2022, will collect data of Jupiter and three of its largest moons, including Europa. Europa Clipper, which will perform reconnaissance of Europa while orbiting Jupiter, is currently under development at NASA. There is also a conceptual study

led by JPL, NASA (Hand et al., 2017) for a Europa Lander Mission that is to search for life on Europa and explore its geology using in-situ techniques.

Raman spectroscopy is an analytical technique which is a promising instrument for life detection on Europa and it is indicated in the Europa Lander Concept report as an instrument potentially capable of achieving the mission's goals (Hand et al., 2017). It is an emerging technology for in-situ space exploration which has until recently been restricted to applications on Earth due to size limitations. Recent advances in optics and laser technology have allowed Raman spectroscopy to be considered for extraterrestrial applications and in 2020 it was launched for the first time on the Mars 2020 mission to search for organics and minerals in the martian soil (Bhartia et al., 2021; Farley et al., 2020). However, most research into adapting Raman spectroscopy for space exploration have been focused on Mars, the most imminent planetary target (Abbey et al., 2017; L. Beegle et al., 2015; Clegg et al., 2015; Rull et al., 2017; Tarcea et al., 2007). While there are now attempts at optimizing the technique for the exploration of Europa (Gasda et al., 2021; J. Lambert & Wang, 2019; Phillips-Lander et al., 2019; Prieto-Ballesteros et al., 2011; Rodriguez-Manfredi et al., n.d.), there are still many challenges to be addressed. Among other potential hurdles, the harsh environmental conditions on Europa are very different to the environment on Mars or Earth and the impact of these conditions on the instruments and the resulting spectral data still needs to be fully assessed and understood.

Intense radiation, extreme low temperatures as well as low concentrations of molecules in an ice matrix could have a significant impact on Raman instruments and the spectra obtained which also bears severe implications on the instrument design (Chyba & Phillips, 2001; Hand et al., 2017; Krajewski et al., 2018; Nordheim et al., 2018; Prieto-Ballesteros et al., 2011). The impact of these conditions needs to be fully understood to ensure successful employment of this technique on a mission to Europa.

Most notably, the temperature on Europa's surface can reach as low as -233 °C (Ashkenazy, 2016). This is significantly lower than any temperature ever recorded on Earth or Mars. For comparison, the lowest surface temperature recorded in-situ on Earth is -89.9 °C (-98 °C from satellite observation data) in Antarctica (Scambos et al., 2018) and the average martian surface temperature is -63 °C with the lowest recorded temperature being -143 °C in the polar regions as estimated from the Viking Orbiter Infrared Thermal Mapper data. These extremely low temperatures could have a major impact on the measurements and resulting spectral data due to thermally induced changes within the molecular bonds. This could severely impact the effectiveness of Raman Spectroscopy in detecting biosignatures on Europa. However, the effects of extreme low temperatures on Raman spectra can be very molecule specific and remain relatively unexplored in research conducted to date.

The severity and type of the temperature induced changes in the spectra can vary significantly across different molecules. To date, extreme low temperatures have been shown to induce shifting of Raman bands towards lower or higher frequencies as well as changes in Raman band width and intensity (Girardot et al., 2008; Haines et al., 2003; Hibbert et al., 2015; Le Tacon et al., 2006; Sandilands et al., 2015; Sobron & Wang, 2011; Sutherland, 1933). The emergence of new Raman bands in the spectra or the diminishing of specific or all bands have also been reported (Girardot et al., 2008; Haines et al., 2003; Le Tacon et al., 2006; Sobron & Wang, 2011; Sutherland, 1933).

While the Raman spectra of some simple molecules, such as water, and some other inorganic materials not significant for astrobiology have been analysed at a decreased temperature, the data available is very limited (Berg, 2018; Girardot et al., 2008; Haines et al., 2003; Hibbert et al., 2015; Liljeblad et al., 2017; Pershin et al., 2015; Sandilands et al., 2015; Sutherland, 1933). Only a very limited number of molecules relevant to astrobiology have been analysed at low temperatures. Raman spectra of some minerals relevant to planetary exploration have been obtained at temperatures between 21 and -95 °C (Sobron & Wang, 2011). Some organic compounds including organic minerals, carboxylic acids and nitrogen-containing aliphatic and aromatic compounds, which are relevant for the search for extraterrestrial life, have also been studied, however, only in the temperature range from 5 to -25 °C (Jehlicka et al., 2010). Neither of these studies

demonstrate the Raman spectra at an adequate temperature range to simulate the conditions on Europa. At extreme low temperatures relevant to Europa, only very limited data are available on the Raman spectra of compounds relevant to astrobiology including studies of methane, ammonia and some olivines (Sutherland, 1933; Weber et al., 2014).

As the effects of extreme low temperatures on Raman spectra are very specific to a particular molecule, a detailed review of relevant target molecules including important biosignatures for the detection of life on Europa at conditions analogous to the Europan environment is necessary.

This research aims to address this by analysing the effects of extreme low temperatures analogous to the Europan surface and sub-surface on the Raman spectra of some important amino acids that represent traditional biosignatures commonly used for the search for extraterrestrial life (i.e. Glycine, L-Alanine, L-Histidine and L-Tryptophan) (Creamer et al., 2017; Hand et al., 2017). The induced spectral changes at temperatures down to -196 ^{O}C, which are relevant for the exploration of Europa, are described and the impact of these changes on the design and functional requirements of Raman instruments designed for life detection in the Europan icy crust is discussed.

1.1. Europa and its Environment

The solar radiation received by Europa is less than 5% of the solar radiation on Earth (Prieto-Ballesteros et al., 2011). As a result of this, the surface of Europa could reach temperatures as low as -233 ^{O}C at the polar region (Ashkenazy, 2016) with the temperature of the Europan surface never rising above -168 ^{O}C (Ashkenazy, 2016). Below the surface, the temperature in the Europan ice shell is expected to rise drastically with increasing depth and at 5 km below the surface the ice shell could reach temperatures between -98 ^{O}C and -75 ^{O}C (Nimmo & Manga, 2004; Tobie et al., 2003). At the depth of 10 km the temperature could be as high as -33 ^{O}C (Nimmo & Manga, 2004; Tobie et al., 2003). The temperature between 10 to 20 km below the surface is thought to stay approximately constant at around -13 ^{O}C until it reaches the water-ice surface where the temperature is believed to be 0 ^{O}C (Nimmo & Manga, 2004; Tobie et al., 2003).

The temperatures relevant for a lander mission to Europa would be the temperatures of the ice at around 10 cm below the surface as that is the minimum sampling depth outlined by the Europa Lander Concept Mission currently under development at NASA (Hand et al., 2017). This is because 10 cm below the surface is the minimum depth at which any potential biosignatures would be protected from the destructive radiation on the surface of Europa (Nordheim et al., 2018). At the dept of approximately 10 cm below the surface, the temperature

could be expected to be roughly -175 ^{O}C (Ashkenazy, 2016; Nimmo & Manga, 2004). Considering that the instrument on board of a lander would receive a conserved sample, the minimum temperature of a sample that the instrument should be able to analyse is -175 ^{O}C. This could be higher or lower depending on the location of the sampling site and the time of day and it could converge towards temperatures around -200 ^{O}C at polar regions or if the desired sampling depth is not achieved. A mole probe mission to Europa that could potentially reach lower layers of the Europan icy crust could then experience higher temperatures depending on the depth of sampling. However, even if the probe reaches the depth of 5 km, which is approximately as deep as the thickest ice sheet on Earth (Fretwell et al., 2013) and could be quite challenging for a space probe, the temperature at this depth could still be below any temperature ever recorded on Earth to date (Scambos et al., 2018).

2. Materials and Methods

The Raman spectra of important amino acids representing potential biosignatures for the search for life on Europa are compared at room temperature (22 ^{O}C) and at extreme low temperatures analogous to the Europan surface and sub-surface (-196 ^{O}C and -100^{O}C). The selection of these temperature reference points as well as representative biosignatures is described further in this section. An analysis of the Raman spectra of Glycine taken at four additional temperature reference points

within this temperature range (-20 ^{O}C, -60 ^{O}C, -132 ^{O}C, -164 ^{O}C) is also included to ensure a more complete understanding of the trends and profiles observed.

L-Alanine, Glycine, L-Histidine and L-Tryptophan were selected as potentially biogenic amino acids that could signal the presence of life on Europa to represent traditional biomarkers for extraterrestrial exploration. Out of the 20 essential amino acids commonly used as biomarkers of extraterrestrial life (Creamer et al., 2017; Hand et al., 2017), L-Tryptophan is used as it is mildly fluorescent at the 785 nm excitation wavelength used in the experiments, which allows observation of the impact of the extreme low temperature on the fluorescence background. Compared to other amino acids, Glycine is the simplest amino acid with no chirality and Alanine is the second simplest, after Glycine, but includes an additional methyl side chain that could provide more information on the relationship of the spectral changes at low temperatures and the molecular structure. Similar to L-Tryptophan, L-Histidine includes an aromatic ring but does not show any fluorescence at 785 nm. It also has a complex Raman spectra with a large number of Raman bands, which can provide more insight into the thermally induced spectral changes. Samples of Glycine (powder, purity >99%) and L-Histidine (powder, purity >99%) were purchased from Sigma Aldrich, L-Alanine (powder, purity >99%) and L-Tryptophan (powder, purity >99%) were obtained from Alfa Aesar.

Measurements were taken with a Raman Renishaw Spectrometer at a 785 nm excitation wavelength. A Linkam THMS600 temperature controlled stage with a liquid nitrogen cooling system was used to cool the samples to -100 ^{O}C, which represents the temperature at the depth of 5 km within the Europan icy shell (Nimmo & Manga, 2004; Tobie et al., 2003) and serves as a gauge measurement, and -196 ^{O}C, which represents the temperature on the Europan surface or near sub-surface (Ashkenazy, 2016; Nimmo & Manga, 2004). The temperature of -196 ^{O}C was chosen as it is likely to be similar to the temperature extremes experienced at 10 cm below the surface which is the minimum sampling depth of the proposed Europa Lander Mission developed by NASA (Ashkenazy, 2016; Hand et al., 2017; Nimmo & Manga, 2004). The measurement at -100 ^{O}C serves as a gauge measurement that provides information about the profile of spectral change with decreasing temperature and the depth within the icy shell. All measurements were performed in a nitrogen purged environment. The temperature rate of change of the cooling stage was set to 55 ^{O}C /minute, and a dwell time of 6 minutes was applied after reaching the measurement temperature to ensure the sample was fully cooled to the required temperature.

Three 10 second measurements at three different laser power settings were taken of each sample and at each temperature to increase statistical confidence in the collected data and their analysis and to observe the spectral variance between individual readings at the same temperature. The nominal laser power at sample

of the 785 nm Raman system was 115 mW and the spectra of L-Alanine and L-Tryptophan were collected at laser power at sample of 5.75, 11.5 and 57.5 mW. The spectra of Glycine were obtained at laser power at sample of 1.15, 5.75 and 11.5 mW and the spectra of L-Histidine at 11.5, 57.5 and 115 mW. The spot diameter of the laser beam was 7.98 μm and approximately 10 mg of each sample was used with an average layer thickness of 0.5 mm. The collected spectra of each sample and at each temperature are compared to identify and quantify the effects of the extreme low temperatures analogous to Europa. Peak fitting is used for the identification of the spectral shifts and Full Width Half Maximum (FWHM) of the peaks is used to assess the width of the Raman bands. The spectral resolution of the 785 nm Renishaw Raman system is 0.57 cm^{-1} to 0.30 cm^{-1} (FWHM).

Monitored effects include shifts in the Raman band position, width and shape as well as emergence of new Raman bands or changes in the overall signal intensity. Any potential effects on fluorescence and background noise in the spectra are also recorded. The significance of the observed spectral shifts and band width changes at low temperatures is assessed using 1σ (32% error probability), 2σ (4.6% error probability) and 3σ (0.3% error probability) error bars calculated for each Raman band over the three measurements at three different power settings. The profile of the spectral changes as a function of temperature is characterized and discussed and the overall effect of the extreme low temperatures on the sample identification is presented. The impact of the extreme low temperatures on design

requirements and the effectiveness of Raman Spectroscopy for life detection on Europa is considered, summarized and discussed.

3. Results

3.1. Glycine

The Raman spectra of Glycine obtained at various temperatures ranging from room temperature (22 ^{O}C) to -196 ^{O}C are shown in Figure 1. As displayed in this figure, Raman bands of Glycine shift to higher frequencies with decreasing temperature. The comparison of the Raman bands at room temperature, -100 ^{O}C and -196 ^{O}C is shown in Table 1. As a result of these shifts, some Raman bands nominally not resolvable at room temperature can be detected at lower temperatures. Most notably, Raman band nominally at 497 cm^{-1} that appears as a single wide Raman band at 22 ^{O}C, visibly splits into two separate Raman bands, 491 cm^{-1} (CH_2 rocking) and 509 cm^{-1} (CCO scissoring), at -20 ^{O}C and becomes fully resolvable as two separate Raman bands at -100 ^{O}C. This is highlighted with an arrow in Figure 1. Similarly, Raman bands at around 185 cm^{-1} and 196 cm^{-1} that blend with the Raman band at 163 cm^{-1} (all associated with NH_2 torsion) and are not individually resolvable at room temperature also show better definition at decreased temperatures. The Raman band at 196 cm^{-1} can be first detected at -20 ^{O}C and is fully resolvable at -196 ^{O}C. Likewise, first detectable at -100 ^{O}C, the emerging Raman band at 185 cm^{-1} continues to separate and become more

defined with decreasing temperature, however, it was not fully resolved within the measured temperature range.

In addition to the Raman band drift to higher frequencies, a significant narrowing of the Raman bands and an increase in intensity of the bands were observed. This also contributed to a better resolution of the spectra at lower temperatures and led to the detection of previously unresolvable Raman bands.

Figure 2 shows the profile of the Raman shift of the 1331 cm^{-1} (asymmetrical stretching of CCO) and 895 cm^{-1} (NH_2 wagging) bands, the two most dominant bands in the Glycine spectra, at decreasing temperature, as well as the profile of the Raman band width narrowing. Other Raman bands of Glycine show similar trends.

As displayed in Figure 2, the Raman bands shift towards higher frequencies with decreasing temperature and the rate of change decreases significantly towards the lowest measured temperature. All Glycine Raman bands shifted towards higher frequencies except for the Raman band nominally at 497 cm^{-1} (CH_2 rocking), which shifted towards lower frequencies with decreasing temperature. However, this is likely due to the split of the 497 cm^{-1} band into two separate bands at lower temperatures as the centre Raman shift of the two blended peaks at room temperature would have been detected in between the Raman shift of the two individual peaks.

The maximum measured shift difference between the room temperature and -196 ^{O}C Raman spectra was 24.97 cm^{-1} (509 cm^{-1} Raman band CCO scissoring) and the minimum 1.16 cm^{-1} (1446 cm^{-1} Raman band assigned to CH_2 scissoring). Both are well beyond the room temperature 3σ error threshold (1.21 cm^{-1} and 0.21 cm^{-1} respectively). This indicates that even the minimum shift difference measured in the Glycine spectra is a significant change that cannot be attributed to variability in the spectra or instrumental error. However, the maximum shift difference was likely measured higher than the true shift difference as a result of the nominal room temperature shift of 509 cm^{-1} band being lower than its true room temperature shift whilst merged with the 497 cm^{-1} band. All changes in the Raman shift observed at -196 ^{O}C were greater than the room temperature 3σ error thresholds of the corresponding Raman bands. This indicates that the observed changes including minimal changes of less than 2 cm^{-1} are unlikely to be the result of variability between measurements and can be assigned to thermal effects.

Bands that on average shifted to higher frequencies at low temperatures by more than 2.6 cm^{-1} (and up to the overall measured maximum of 24.97 cm^{-1}) were all associated with vibrational modes involving the molecule extremities, that is, the NH_2 group or the COO group, or vibrations along the entire main chain of the molecule, that is, NCC bending, or a significant part of it, that is, CCO or CC=O bending. All Raman bands that shifted to lower frequencies at low temperatures or higher frequencies but only by a relatively small amount (<2.4 cm^{-1}) compared

to other bands (note that the absolute minimum positive shift was 1.16 cm^{-1} as stated previously) were predominantly associated with stretching vibrational modes or vibrational modes involving the inner atom of the molecule (CH_2). No band solely assigned to a stretching vibration increased in frequency at lower temperature by more than 2.36 cm^{-1}.

The change of the Raman band width with temperature, as shown in Figure 2, demonstrates a significant narrowing of the Raman band width at lower temperatures. Similarly to the Raman shift, the rate of change decreases towards the lowest measured temperature. The maximum measured Raman band width difference between that at room temperature and at -196 ^{O}C measurements was 24.67 cm^{-1} at 497 cm^{-1} (CH_2 rocking), which corresponds to a 80.14% change in width and falls well beyond the room temperature 3σ error threshold of 1.48 cm^{-1}. The minimum Raman band width difference between the temperature extremes was 1.9 cm^{-1} (895 cm^{-1} band mostly attributed to NH_2 wagging) which is a 24.72% change from the nominal room temperature band width and also significantly higher than the 3σ error threshold of 0.62 cm^{-1} for this particular band. Similar to the Raman shift, the changes observed in the width of the Raman bands at -196 ^{O}C across all Glycine bands were greater than the corresponding 3σ error thresholds. This indicates that the observed narrowing of the Raman bands is too significant to be attributed to variability in the measurements or instrumental error.

Both the Raman shift and width data suggest that there is a relationship between the temperature and the level of variance between the individual spectra obtained at each temperature reference point, as the individual measurements seem to show less variance at lower temperatures. This is also clearly visible in the band shift and width profiles at 1331 cm^{-1} and 895 cm^{-1}, as displayed in Figure 2.

To visualize and characterize this occurrence, the average variance of individual spectra across all Glycine Raman bands was plotted against the temperature at which the spectra was obtained, as shown in Figure 3. The figure shows a clear linear decrease in the shift variance with decreasing temperature. The Raman band width data also indicates a decrease in the width variance at lower temperatures, however, this relationship is not as clear and does not show a strong linear relationship. This is possibly due to experimental discrepancies or the width measurements being more susceptible to discrepancies due to handling, environmental or material differences within the sample.

While the average Raman shift variance between different measurements at room temperature can be as high as 0.157% compared to the average value, at -196 ^{O}C the average Raman shift variance drops to 0.041%.

Likewise, at 22 ^{O}C the average Raman band width variance across all Glycine Raman bands is 7.54%. At -196 ^{O}C the variance decreases to 5.669%. In this case, the average width variance at -20 ^{O}C (i.e., 16.764%) breaks away from the

decreasing pattern as it is far greater than the variance at room temperature. The data shows that this significant fluctuation is the result of an abnormally low measurement of the 1417 cm^{-1} band (NH_2 and CH_2 torsion) width at -20 ^{O}C and inconsistent measurements of the same band at room temperature most probably caused by experimental discrepancy during the measurement.

The relationship between the Glycine spectra intensity and the temperature was found to be too inconsistent to derive a definitive profile, however, there is a visible increasing trend towards lower temperatures. All 15 fully detectable Glycine Raman bands show an increase in their intensity at -196 ^{O}C compared to the room temperature measurement. The Raman signal intensity change between room temperature and -196 ^{O}C across Glycine Raman bands is shown in Figure 4. The lowest increase in intensity was 5.5% at 509 cm^{-1} (CCO scissoring), however, the intensity increase data in this case could be inaccurate due to the split of 509 cm^{-1} from 497 cm^{-1} below room temperature. The second lowest increase in intensity, 6.1%, was detected at 1446 cm^{-1} (CH_2 scissoring) and might be a more accurate representation of the intensity increase minimum within Glycine spectra at -196 ^{O}C. The maximum intensity increase between room temperature and -196 ^{O}C was 67.8% at 497 cm^{-1} (CH_2 rocking), which could have also been affected by the split of 509 cm^{-1} from 497 cm^{-1}. The second highest increase in intensity was 45% at 1144 cm^{-1} (mostly assigned to NH_2 wagging), which might be more representative of the potential maximum increase in intensity. The average

increase in intensity across all Glycine Raman bands was 26.5% and while the intensity increase is band specific and does not accurately describe the overall trend, it might still have some level of statistical value as a general guideline for the Raman signal intensity increase that could be expected at -196 ^{O}C.

3.2. L-Alanine

Raman spectra of Alanine was obtained at 22 ^{O}C, -100 ^{O}C and -196 ^{O}C and the comparison of the spectra is shown in Figure 5. As shown in the figure, a shift of Alanine Raman bands to higher frequencies was observed at lower temperatures, however, this shift was not as consistent as in the Glycine spectra discussed earlier. Additionally, some Alanine bands also shifted to lower frequencies. The Raman band assigned to NH_2 and CH_3 rocking nominally at 283 cm^{-1} at room temperature moved to 274 cm^{-1} at -100 ^{O}C and then to higher frequency of 285 cm^{-1} at -196 ^{O}C again. Similarly, 654 cm^{-1} band (NCC=O bending) moved to 653 cm^{-1} at -100 ^{O}C and then 655 cm^{-1} at -196 ^{O}C. The average shift change from room temperature to -196 ^{O}C in this case was exactly 1 cm^{-1}, which is within the 3σ error region (0.88 - 1.33 cm^{-1}), which indicates that there is only a negligible probability of these measurement being the result of variability in the data or an error rather than the result of thermal changes within the spectra. Likewise, the Alanine band at 775 cm^{-1} (C-COOH stretching) at room temperature moved to 774 cm^{-1} at -100 ^{O}C where it remained also at -196 ^{O}C. The average shift decrease

from room temperature to -196 ^{O}C in this case was 1.6 cm^{-1}, which is beyond the 3σ error threshold of 1.11 cm^{-1} for this band and thus also very unlikely to be an outlier or an error in the data.

Similarly to the spectra of Glycine, the Alanine spectra also shows new Raman bands emerging at lower temperatures that were not visible or detectable at room temperature. While visible at room temperature and -100 ^{O}C, the Raman band at 146 cm^{-1} (COOH torsion) is only fully resolvable at -196 ^{O}C. At -100 ^{O}C, a small peak at 227 cm^{-1} appears in the spectra and seems to gain more intensity as it travels to 232 cm^{-1} at -196 ^{O}C. While this peak is too weak to be resolvable, it is clearly visible in the spectra at lower temperatures. Similarly, the broad Raman band at 328 cm^{-1} (mixed vibration of CH_3 rocking and CCN bending) seems to diminish at -100 ^{O}C and two very weak bands at 322 cm^{-1} and 340 cm^{-1} take its place. While the 322 cm^{-1} band is too weak to be detectable, the 340 cm^{-1} band appears stronger and becomes very clearly distinguishable at -196 ^{O}C as it shifts to 346 cm^{-1} and gains more intensity.

Interestingly, the Alanine 283 cm^{-1} band (NH_2 and CH_3 rocking), which appears as a single wide band at room temperature, splits into 3 separate peaks at -100 ^{O}C, which then become even more defined at -196 ^{O}C as the intensity of the middle peak rises. Only the middle peak is fully resolvable.

While the most dominant Raman band of Alanine, 854 cm^{-1} (C-CH_3 stretching), and most other Alanine bands follow the same general Raman shift and width pattern as Glycine bands (as shown in Figure 6), this is not necessarily the case for all Alanine Raman bands. As already mentioned, not all the Alanine bands shifted to higher frequencies and while most bands show a decreasing rate of change in the Raman shift and width at decreasing temperature, the profile is not as consistent as with the spectra for Glycine. For comparison, Figure 6 shows the Raman shift and width profile of the 283 cm^{-1} band which shifts to a lower frequency at -100 ^{O}C and higher again at -196 ^{O}C.

Across all Alanine Raman bands the minimum change between the room temperature and -196 ^{O}C Raman shift was 0.92 cm^{-1} at 532 cm^{-1} (COH torsion). The maximum change was 18.78 cm^{-1} and it occurred at 328 cm^{-1} (mixed vibration of CH_3 rocking and CCN bending). Both of these sifts lie beyond the 3σ error threshold for these peaks, 0.46 cm^{-1} and 3.74 cm^{-1} respectively. Overall, the recorded changes in shift from room temperature to -196 ^{O}C were beyond the 3σ region for all Alanine Raman bands except for the 654 cm^{-1} band (NCC=O bending), where the recorded shift lies within the 3σ region, and the 1416 cm^{-1} band (CH_3 bending), where the recorded shift falls within the 2σ region. While this signals greater variability in the data than in the spectra of Glycine, it also indicates at least 99.7% confidence (95.4% for the 1416 band cm^{-1}) than none of the recorded shift changes are the result of an error or variability in the data.

Similar to the bands of Glycine, all Alanine bands that on average shifted to higher frequencies at low temperatures by more than 1.6 cm^{-1} (and up to the overall measured maximum of 18.78 cm^{-1}) are associated with vibrations of the outside parts of the molecule, that is, its methyl side chain (CH_3) and its amine functional group (NH_3), or vibrations along the length of the main molecule chain, that is, CCO, CCC or CCN bending. The only shift that decreased in frequency at low temperatures is assigned to a stretching vibrational mode and none of the alanine bands solely assigned to a stretching vibration increased in frequency by more than 1.42 cm^{-1} at low temperatures.

Despite some inconsistencies in the data, a general trend of Raman band narrowing at decreasing temperature was observed. The minimum Raman band width across all Alanine bands was measured at the 1489 cm^{-1} band at all temperatures; 5.81 cm^{-1} at 22 ^{O}C, 4.36 cm^{-1} at -100 ^{O}C and 4.18 cm^{-1} at -196 ^{O}C. The maximum Raman band width at room temperature was 15.82 cm^{-1} at 1153 cm^{-1}. At -100 ^{O}C it was 18.79 cm^{-1} measured at the 274 cm^{-1} Raman band and 11.64 cm^{-1} at -196 ^{O}C at the Raman band of 1417 cm^{-1}.

The minimum measured difference between the Raman band width between room temperature and -196 ^{O}C was exactly 1 cm^{-1} at 1468 cm^{-1} (CH_3 bending) which corresponds to a 14.3% change from the nominal room temperature value. While this is a minimal change within the spectra, it lies beyond the 3σ error threshold of

0.21 cm^{-1} for this peak. The maximum Raman band width change was 12.18 cm^{-1} at 283 cm^{-1} (62.4%) attributed to NH_2 and CH_3 rocking, however, in terms of the highest change in percentage to the nominal value it was 64.7% at 481 cm^{-1} (CCO bending) which was 10.67 in cm^{-1}. Overall, most changes recorded in the width of Alanine Raman bands were beyond their corresponding 3σ error thresholds, only the width change recorded at the 328 cm^{-1} and 481 cm^{-1} bands was within the 3σ error range, and 922 cm^{-1} and 1365 cm^{-1} bands within the 2σ error range. While this signals higher variance in the width change data than the shift change data, it still indicates a high confidence in the width change being the result of the thermal changes rather than any discrepancy in the data.

Just like in the case of Glycine, the average variance of the individual Raman shift measurements across all fully detectable bands decreases at lower temperatures showing a clear linear relationship, as displayed in Figure 7. The average variance across all peaks at room temperature is 0.072% from the nominal value while at -196 ^{O}C the variance drops to 0.050%. Similar to Glycine, the Raman band width variance across individual measurements is less consistent than the variance of Raman shift as shown in Figure 7. While it displays a decreasing trend towards lower temperatures, the decrease is almost level and there is no clear linear relationship indicated in the data. At room temperature the band width variance is 10.3% which then decreases to 8.15% at -100 ^{O}C and rises again to 10.15% at -196 ^{O}C. The Raman band width data can be more severely impacted by spectral

changes, such as the emergence of new peaks and severe intensity changes between measurements at various temperatures, as shown in the spectra of Alanine in Figure 5. As such, this discrepancy could be assigned to the varied changes in the Alanine spectra between 22 ^{O}C and -196 ^{O}C.

Similarly, the intensity of the majority of Alanine bands decreased at lower temperatures. This is different to that observed for the Glycine Raman bands, where the intensity increased at lower temperatures. Figure 8 shows the intensity change of all fully detectable Alanine bands from room temperature to -196 ^{O}C. All 19 fully detectable Alanine bands showed a signal intensity decrease. The average decrease in intensity across all bands was 18.2% with the maximum decrease being 35.4% at 283 cm^{-1} (NH_2 and CH_3 rocking) and the minimum 1.5% at 1025 cm^{-1} (mainly attributed to CH_3 torsion). It is also important to note that the intensity of Alanine peaks changes a lot more dramatically with temperature as shown in the spectra in Figure 5. Some bands, such as 398 cm^{-1} (CCN bending), 532 cm^{-1} (COH torsion) and 1489 cm^{-1} (CH_3 bending), decrease in intensity significantly at -100 ^{O}C (beyond their 3σ error threshold) and then visibly rise again compared the rest of the spectra at -196 ^{O}C. The rise in intensity at -196 ^{O}C lies beyond the 3σ error threshold for 1489 cm^{-1} and within the 3σ region for 398 cm^{-1} and 532 cm^{-1}, which indicates that these changes are induced by the varying temperature rather than being the result of variability in the data. Similarly, while the overall intensity of the 481 cm^{-1} band (CCO bending)

decreases, the band is barely detectable at room temperature and becomes increasingly more distinguishable towards lower temperatures even despite the overall intensity decrease.

3.3. L-Histidine

The comparison of Raman spectra of Histidine obtained at room temperature, -100 ^{O}C and -196 ^{O}C is shown in Figure 9. Histidine has a more complex molecular structure than Glycine and Alanine, leading to a more varied Raman spectrum. However, the changes at lower temperatures display similar trends and no other additional effects were observed. A shift to higher frequencies was observed for most Histidine bands with a couple of exceptions; 404 cm^{-1} (CH_2 rocking and out of plane bending of CH_2-CH-NH_2), 966 cm^{-1} (breathing of the ring) and 1145 cm^{-1} (asymmetrical stretching of CH_2-CH-NH_2), that shifted to lower frequencies. Some bands, including 627 cm^{-1} (out of plane deformation of the ring) and 657 cm^{-1} (CH_2-ring stretching), only exhibited very minor Raman shift changes not resulting in any substantial Raman band shifts in the spectra. While the minimal change in the shift of the 657 cm^{-1} band was most likely a result of variance in the spectra (1σ error region), the change recorded in the shift of the 627 cm^{-1} band was within the 3σ error region and thus a result of the thermal change. However, in both cases the data indicates that both of these bands are very thermally stable. Similar to some Alanine bands, the Histidine CH_2

torsion band nominally at 1255 cm^{-1} shifted to 1257 cm^{-1} at -100 ^{O}C and then to 1256 cm^{-1} at -196 ^{O}C. However, in this case this could have also been a result of excessive variance in the spectra. Additionally, the emergence of new bands that were not visible in the spectra at room temperature was recorded. Previously undetectable peaks at 340 cm^{-1} (CH_2 rocking) and 431 cm^{-1} (CC=O bending) appear in the spectra at -100 ^{O}C and become more distinguishable at -196 ^{O}C as they shift to 431 cm^{-1} and 435 cm^{-1} respectively. Moreover, the band clearly visible at 213 cm^{-1} at room temperature becomes unresolvable at -100 ^{O}C and -196 ^{O}C as it fades and blends with the 240 cm^{-1} band, both assigned to CH_2-ring and C-NH_2 bending.

Most Histidine bands display similar change profiles in Raman shift and width with decreasing temperature, as already described in Figure 2 and Figure 6 (a and c) for Glycine and Alanine. The profile of the Raman shift and width change as a function of temperature for the most dominant Histidine Raman band at 1323 cm^{-1} (mixed vibration of CH_2 wagging and ring breathing) is shown in Figure 10. While most Histidine bands displayed a similar profile, there were some exceptions as some bands shifted to lower frequencies or diminished at lower temperatures all together as described above.

The minimum change in the Raman shift between room temperature and -196 ^{O}C across all Histidine bands was 0.35 cm^{-1} at 1276 cm^{-1} (mixed vibration of CH_2

wagging, CH bending and ring breathing). This shift lies in the 3σ error region, which indicates that the change is highly unlikely to be attributed to variance in the spectra and represents a genuine thermally induced change. Nevertheless, this minimal change also signals that the 1276 cm^{-1} band is very thermally stable. The maximum Raman shift change was 8.79 cm^{-1} at 135 cm^{-1} (ring-CH_2-CH bending). While some Histidine Raman bands were undetectable at room temperature and error bars could not be generated, the shift change of all fully detectable bands except for 5 were greater than their 3σ error thresholds, 4 were within the 3σ error region and, as discussed earlier, the 657 cm^{-1} band was within 1σ error region but only very minor change was recorded.

Unlike Glycine and Alanine, the Histidine molecule has an imidazole ring in its structure, however, the observed trends in the thermally induced shifts of its vibrational modes were similar. All the Histidine bands that on average shifted to higher frequencies at low temperatures by more than 3.5 cm^{-1} (and up to the overall measured maximum of 8.79 cm^{-1}) were assigned at least partially to vibrational modes involving the molecule's outer atoms, that is, the amine group (NH_2) or the carboxylic acid group (COOH), or bending along the length of the molecular chain, that is, bending of the ring and CH_2 or bending of the ring or the carboxylic acid group against CH_2-CH. Bands associated with in plane bending within the imidazole ring also displayed shifts to higher frequencies greater than 3.5 cm^{-1}. Histidine bands that displayed a shift to lower frequencies at low

temperatures or that shifted to higher frequencies only by less than 0.55 cm^{-1} were predominantly assigned to stretching vibrational modes, that is, stretching between individual atoms as well as ring breathing or ring in plane deformation, or vibrational modes including inner atoms of Histidine (CH_2 or CH). None of the bands assigned to out of plane ring deformation generated shifts to higher frequencies at low temperatures greater than 0.82 cm^{-1}. None of the bands solely or predominantly assigned to stretching vibrations shifted to a higher frequency by more than 1.4 cm^{-1}.

As already observed with Glycine and Alanine, Raman band width narrowing was observed in the spectra of Histidine at low temperatures. The decrease in Raman band width from room temperature to -196 ^{O}C was as high as 15.45 cm^{-1} at 922 cm^{-1} (N=CH-NH scissoring in the ring) which roughly corresponds to 67.92% of the room temperature width. The minimum change in the Raman band width was 1.03 cm^{-1} (15.26%) as observed at 1436 cm^{-1} (CH-NH stretching in the ring) or 4.36% (1.21 cm^{-1}) at 627 cm^{-1} (out of plane deformation of the ring), both within the 3σ error region. Overall, most fully detectable Raman bands displayed changes in the band width greater than their 3σ error thresholds, however, 5 bands were within the 3σ error region and 1 in the 2σ error region. This signals a high probability that all the recorded changes can be attributed to the temperature decrease rather than variance in the data. Compared to Alanine and Glycine, Histidine bands in general are narrower and potentially more restrictive in terms

of spectral resolution for successful detection. At room temperature the narrowest band is 1.81 cm^{-1} wide at 1065 cm^{-1}, at -100 ^{O}C it is 2.65 cm^{-1} at 404 cm^{-1} and at -196 ^{O}C it is 2.66 cm^{-1} at 1116 cm^{-1}.

The variance between individual Histidine Raman spectra at each measured temperature is summarized in Figure 11. Across all Histidine bands the variance of the Raman shift decreases linearly with decreasing temperature, which corresponds to the Glycine and Alanine variance trend described previously. From a variance of 0.041% at room temperature, the Raman shift variance drops to 0.033% at -100 ^{O}C and 0.022% at -196 ^{O}C.

While there is a clear decreasing trend in the Raman band width variance across all fully detectable Histidine bands towards lower temperatures, the relationship is not as clearly linear as the Raman shift variance profile. As shown in Figure 11, the band width variance at room temperature is 8.43%, rising slightly to 8.996% at -100 ^{O}C and then dropping to 7.208% at -196 ^{O}C.

Overall, most Histidine bands displayed higher intensity at -196 ^{O}C than at room temperature. As shown in Figure 12, out of 24 fully detectable bands, 15 increased and 9 decreased in intensity at -196 ^{O}C compared to 22 ^{O}C. The average intensity change across Histidine bands was a 2.05% increase, however, the maximum change was a 37% decrease at 135 cm^{-1} (ring-CH_2-CH bending) and the minimum change was a 25.22% increase at 404 cm^{-1} (CH_2 rocking and out of

plane bending of CH_2-CH-NH_2). Additionally, as discussed above, the 213 cm^{-1} Histidine band diminishes at lower temperatures all together and 340 cm^{-1} and 431 cm^{-1} bands emerge in the spectra at -100 ^{O}C and become more distinguishable as they further intensify at -196 ^{O}C.

3.4. L-Tryptophan

The Raman spectra of Tryptophan obtained at room temperature, -100 ^{O}C and -196 ^{O}C are compared in Figure 13. While most bands shift to higher frequencies at lower temperatures as previously observed in the spectra of Glycine, Alanine and Histidine, the 164 cm^{-1} (out of plane deformation of the indole rings) and 1256 cm^{-1} (CH_2 wagging and indole breathing) bands shift to lower frequencies and the 1464 cm^{-1} (in plane indole deformation) and 1565 cm^{-1} (CH=C stretching in the pyrrole ring) bands shift to a higher frequency at -100 ^{O}C and then lower again at -196 ^{O}C. Additionally, some bands only shift by a very small amount. Namely, the 1012 cm^{-1} band (CH=CH stretching in the benzene ring) shifts to a lower frequency and the 842 cm^{-1} (benzene ring CH torsion) and 1494 cm^{-1} (in plane indole deformation) bands shift to higher frequencies, but the changes do not exceed 0.7 cm^{-1}. Although minimal, these changes correspond to values higher than the 3σ error region, the 3σ error region and the 2σ error region respectively, and as such cannot be disregarded as variance in the data. This also indicates that these bands are relatively thermally stable. In general, changes in

the Raman shift across Tryptophan bands at lower temperatures are relatively minor compared to changes observed in the spectra of Glycine, Alanine and Histidine. The maximum measured shift from room temperature to -196 ^{O}C was 7.95 cm^{-1} at 123 cm^{-1} (in plane bending of the entire molecule) and the minimum measured shift of 0.45 cm^{-1} was at 757 cm^{-1} (benzene and pyrrole ring breathing). This change in the shift lies beyond the 3σ error threshold for this band and as such it indicates that the change is a result of the temperature decrease rather than variability in the data and that the band is thermally exceptionally stable. Among all Tryptophan Raman bands, the recorded changes in the shift are greater than the 3σ error threshold in most cases with 3 bands in the 3σ error region and 2 in the 2σ sigma error region. This provides high confidence that all recorded changes in the shift can be attributed to thermal effects rather than variability in the data.

No new Raman bands were detected emerging in the Tryptophan spectra at lower temperatures.

The molecule of Tryptophane includes an indole group composed of a benzene and pyrrole ring and the thermally induced shifts of its vibrational modes displayed similar trends observed in the spectra of Histidine. Similar to all the other examined amino acids, all Tryptophane Raman bands that shifted to higher frequencies the most at lower temperatures (by >1.77 cm^{-1} and up to the absolute overall measured maximum of 7.95 cm^{-1}) were either assigned to the vibrations of

the outer parts of the Tryptophan molecule, that is, its amine group, or vibrational modes including the entire molecule or most of its main chain, that is, bending of the indole group against the carboxylic acid group. Raman bands that either shifted to lower frequencies at lower temperatures or shifted to higher frequencies by less than 0.83 cm^{-1} were predominantly assigned to stretching vibrational modes, that is, stretching between individual atoms as well as in plane deformation of the ring or ring breathing, or vibrational modes associated with the inner atoms of the molecule, that is, CH_2 or CH, or out of plane deformation of the rings. The only band that shifted to a lower frequency by more than 2 cm^{-1} was assigned to out of plane deformation of the indole group. Additionally, similarly to Histidine, none of the bands associated with out of plane deformation of the rings shifted to higher frequencies at low temperatures by a significant amount compared to other Histidine bands (<1.18 cm^{-1}). This is also true for any bands associated with stretching vibrational modes which did not shift to higher frequencies by more than 1.44 cm^{-1}.

While no fluorescence was detected in the spectra of Glycine, Alanine and Histidine, a clear fluorescence background is visible in the Tryptophan spectra at all measured temperatures. As shown in Figure 13, the fluorescent background becomes more pronounced at lower temperatures and intensifies as the temperature decreases. As displayed in Figure 14, this is also reflected in the average Signal to Noise (S/N) ratio calculated for one of the most dominant

Raman bands at 1012 cm^{-1} compared to the fluorescence background at 450 cm^{-1}. The S/N ratio drops linearly with decreasing temperature at the rate of 0.2786 K^{-1}.

The profile of the Raman shift and width change as a function of temperature for one of the most dominant Tryptophan bands at 757 cm^{-1} (benzene and pyrrole ring breathing) is shown in Figure 15. In general, all other Tryptophan bands that shift to higher frequencies at lower temperatures follow a similar pattern. A similar pattern was also observed for other analysed amino acids as discussed previously with a notable difference of the Tryptophan band width profile being more inconsistent and resulting in a more linear decrease. For comparison, image b and c in Figure 15 show the Raman shift and width change profile of band 164 cm^{-1} (indole out of plane deformation) which shifts to lower frequencies with decreasing temperature. As shown in the figure, the 164 cm^{-1} profile of Raman shift and width change is approximately an inverse of the profile of the bands that shift to higher frequencies, as displayed in Figure 2, Figure 6 (a and b), Figure 10 and Figure 15 (a and b).

Just like the spectra of other examined amino acids, Tryptophane bands show significant narrowing at lower temperatures, however, the data is not as consistent which might be partly a result of the fluorescence background. The overall maximum change in the band width from 22 ^{O}C to -196 ^{O}C was 10.95 cm^{-1} at 877 cm^{-1} (NH_2 wagging and CH_2 rocking) which is 67.76% of the nominal room

temperature width. The minimum change in width across all Tryptophan bands was 0.87 cm^{-1} at 757 cm^{-1} (benzene and pyrrole ring breathing), which is 12.73% of the original width and lies beyond the 3σ error threshold of 0.63 cm^{-1}. This indicates that even this minor change can be attributed to the temperature decrease rather than variability in the data. Similar to the changes recorded in the Tryptophan band shift, the changes in the band width were also greater than the 3σ error threshold in most cases with 2 bands in the 3σ error region and 3 bands in the 2σ error region. While this indicates that the band width data may be more prone to variability in the data than the shift measurements, it still provides sufficient confidence that all observed changes are the result of the decrease in temperature. At room temperature the minimum band width across all Tryptophan bands was 4.20 cm^{-1} at 1494 cm^{-1}, at -100 ^{O}C it was 3.64 cm^{-1} at 842 cm^{-1} and at -196 ^{O}C it was 3.16 cm^{-1} at 1494 cm^{-1}.

The variance between individual Tryptophan Raman measurements as a function of temperature is shown in Figure 16. Both the Raman band shift and width variance show a decreasing trend at lower temperatures. However, the relationship is not linear as observed for other analysed amino acids. At room temperature the Raman shift variance is 0.078%, which then drops to 0.031% at -100 ^{O}C and rises again to 0.066% at -196 ^{O}C. The same pattern is observed for the variance in the band width as the width variance drops from 17.78% at room temperature, to 9.90% at -100 ^{O}C, just to rise again to 16.03% at -196 ^{O}C. In this

case it should be noted that the presence of fluorescence might have impacted the variance data.

The change in intensity across all fully detectable Tryptophan bands from 22 ^{O}C to -196 ^{O}C is shown in Figure 17. Of the 16 fully detectable bands, half decrease in intensity at lower temperatures and the other half increase. The highest intensity increase was 25.1% at 842 cm^{-1} (benzene ring CH torsion) and the highest decrease was 30.5% at 708 cm^{-1} (indole out of plane deformation). However, as shown in Figure 17, the intensity of most bands did not change from room temperature to -196 ^{O}C by more than 10% and the average intensity change was a 3% decrease. While the increase in the fluorescence background affects the detectability of individual Tryptophan bands, no bands completely diminished at lower temperatures.

4. Discussion

The results of this study show common trends in the spectral changes of the analysed amino acids induced by exposure to extreme low temperatures. These include the shifting of Raman bands to higher frequencies, Raman band narrowing and decreasing variance between individual measurements. Other changes observed, such as the emergence or diminishing of Raman bands, shifting

of Raman bands towards lower frequencies, increased levels of fluorescence or changes in the signal intensity, were found to be specific to a particular molecule.

The most dominant Raman shift change among all amino acids was a shift to higher frequencies at lower temperatures. This shift is caused by the strengthening of the molecular bonds at these lower temperatures making the bond more rigid and thus causing it to vibrate at a higher frequency. The profile of this change was similar across most Raman bands in all amino acid spectra and it can be characterized approximately by a 3rd order polynomial curve. While no measurements were taken at temperatures below 77.15 K, it is reasonable to assume that the curve would converge to a flat line towards 0 K due to the restricted molecule vibrations at these temperatures. This is visualized in Figure 18 (a), which displays the Raman shift and width at temperatures down to 0 K predicted based on the collected experimental data for Glycine.

With the exception of Glycine, the spectra of all measured amino acids also contained bands that shifted to lower frequencies, indicating a relaxation of the molecular bond at lower temperatures. Additionally, some bands in the spectra of Alanine, Histidine and Tryptophan also initially shifted to lower frequencies at -100 ^{O}C and then higher frequencies at -196 ^{O}C. This indicates a structural change occurring within the molecule and its bonds between these temperatures. It also suggests that Raman spectroscopy at extreme low temperatures can be a very

useful tool for material characterisation as it could help diagnose the changes within the molecules as a function of temperature. This could be useful not only for life detection on Europa but also the exploration of Europa in general as well as for a wide spectrum of applications on Earth as it could provide more information about the sampled material and associated environmental or geological processes.

Among all analysed amino acids, Glycine displayed the most significant Raman shift changes from room temperature down to -196 ^{O}C, closely followed by Alanine. Histidine and Tryptophan showed relatively minor changes in the Raman band shift between the two temperatures and the Tryptophan spectra were the least impacted by the extreme low temperature at -196 ^{O}C in terms of Raman band shift changes.

Across all the amino acids examined in this study, the largest Raman band shift change that was observed when comparing spectra at room temperature to those at -196 ^{O}C, was 24.97 cm^{-1} and the smallest was 0.35 cm^{-1}. While these changes are molecule specific and other amino acids could exhibit larger or smaller changes, the range of 0.35 cm^{-1} to 24.97 cm^{-1} could serve as a general guideline of the foreseeable Raman band shift within the spectra of amino acids representing biosignatures for the search for life as collected on Europa at extreme low temperatures. Especially at the higher end of this range, this could be a major

spectral change compared to the spectra obtained at Earth-like conditions and could severely impact the detectability and the analysis of the Raman spectra from samples collected on Europa or other Icy Worlds.

Nevertheless, across the four examined amino acids, most Raman bands except for a few notable exceptions showed relative stability over the measured temperature range. While this may be molecule specific and other molecules relevant to astrobiology need to be examined at extreme low temperatures to make any definitive conclusions, this would indicate that databases of Raman spectra collected at higher terrestrial temperatures can still be useful for the identification of molecular species in the spectra collected at extreme low temperatures analogous to Europa or Enceladus.

A common trend was observed in the thermally induced shifts of the vibrational modes among all the examined amino acids. Raman bands that shifted to higher frequencies at lower temperatures the most were all assigned at least partially to the outer parts of the molecule such as its side chains or outer atoms or bending involving the main chain of the molecule or a significant part of the molecular main chain. For molecules with a ring in its structure, in plane bending within the ring also seems to generate a significant upwards frequency shift at low temperatures compared to the shift of bands associated with other types of vibrations. The actual shift is molecule dependant and dictated by the relative

shift change at low temperatures across all Raman bands within the spectra and as such it is impossible to determine a threshold for these vibrational modes. For Tryptophan, bands associated with these vibrations shifted to higher frequencies by more than 1.77 cm^{-1}, for Histidine 3.5 cm^{-1}, Alanine 1.6 cm^{-1} and Glycine 2.6 cm^{-1}.

Similarly, all bands among all examined amino acids that displayed relatively small upwards change in the Raman shift at low temperatures compared to other bands within the spectra or that shifted to lower frequencies were all assigned to stretching vibrational modes (including ring breathing and in plane deformation for molecules with a ring in their structure), vibrations involving inner atoms of the molecules or out of plane deformation of a ring. While a threshold is impossible to determine, these types of vibrations were associated with all bands that shifted to higher frequencies by less than 0.83 cm^{-1} in the spectra of Tryptophan, 0.55 cm^{-1} in Histidine, 1.42 cm^{-1} in Alanine and 2.4 cm^{-1} in Glycine. Across all examined amino acids, bands associated with stretching vibrational modes dominate among the shifts to lower frequencies and relatively small shifts to higher frequencies compared to other bands in the spectra. Across all the examined amino acids, no band solely or predominantly assigned to a stretching vibration increased in frequency at lower temperature by more than 2.36 cm^{-1}. For molecules with a ring in their structure, out of plane deformation of the ring also displayed relatively small or negative shifts to higher frequencies at low

temperatures. None of the bands associated with out of plane deformation of the rings in the observed spectra of Tryptophan and Histidine shifted to higher frequencies by more than 1.18 cm^{-1}.

This leads to an assumption that bands associated with stretching vibrations, out of plane deformation of a ring or vibrations including inner atoms of a molecule are more likely to shift to lower frequencies at low temperatures or shift to higher frequencies by only a small amount compared to bands assigned to other vibrational modes. This may be the result of these vibrations being relatively well constrained within the structure of the molecule. On the contrary, bands that shift to a significantly higher frequency at lower temperature are more likely to be associated with vibrations that are relatively less constrained within the molecule, that is, vibrational modes including the extremities of a molecule, such as its side chains, outer atoms and groups, or vibrations including most or all of the molecule main chain and in plane bending within a ring.

Additionally, the shifting Raman bands might also affect the spectral resolution necessary for successful detection, which has direct implications on the design of Raman instruments for life detection on Europa. The clearance between individual adjacent bands within Raman spectra of each amino acid was recorded and the minimum clearance for each amino acid at each measured temperature is shown in Table 2. The spectra of Histidine is the most complex among the

measured amino acids and its spectra shows the lowest clearance between individual bands necessary to resolve two adjacent Raman bands. At room temperature the minimum clearance is 12.43 cm^{-1}, at -100 ^{O}C it is 13.91 cm^{-1} and at -196 ^{O}C it is 14.75 cm^{-1}, all within the spectra of Histidine. This suggests that the spectral resolution of a Raman instrument for the detection of biosignatures needs to be higher than these values to fully detect Histidine.

Furthermore, the spectral resolution required to successfully identify amino acids in a mixture of compounds will be higher due to interference of the bands within the spectra. On Earth amino acids occur predominantly in a mixture of various amino acids and without an instrument with an exceptional spatial resolution or employing Surface Enhanced Raman Spectroscopy, this interference may prove to be critical for successful identification and may dictate the required spectral resolution. There are hundreds of known amino acids, however, just among the 4 amino acids examined in this study there are 8 Histidine bands that lie within 14.75 cm^{-1} of at least 1 Glycine band, 7 of a Tryptophan band and 15 of an Alanine band at -196 ^{O}C. This includes dominant Raman bands that are important for identification and as such this spectral resolution would not be sufficient to resolve these amino acids in these mixtures. The number of potentially unresolvable bands of Glycine and Tryptophan in a mixture with Histidine with a 14.75 cm^{-1} resolution is around half of the overall number of their fully detectable Raman bands, for Histidine and Alanine this is 68% of Alanine bands and almost

50% of Histidine bands. The number of potentially unresolvable bands in mixtures of the examined amino acids depending on the spectral resolution is summarised in Table 3 for both room temperature and -196 ^{O}C.

At -196 ^{O}C, there are 4 Histidine bands that lie within 5 cm^{-1} of a Glycine band and that could be potentially unresolvable with spectral resolution less than 5 cm^{-1}. This is 24% of Raman bands within Glycine spectra and 12% within Histidine spectra. While most of these bands are not particularly important for the identification of Histidine, it includes the Histidine 1117 cm^{-1} band which is a relatively dominant band and can be used for the identification of Histidine. This band lies merely 2.74 cm^{-1} from an adjacent Glycine band and it is also the narrowest Raman band among all the examined amino acids at -196 ^{O}C. With a width of only 2.66 cm^{-1}, it could entirely disappear within the considerably wider 1120 cm^{-1} Glycine band (7.74 cm^{-1} width). It is also important to note that the detection of the extremely narrow 1117 cm^{-1} band (1116 cm^{-1} at room temperature) may be even more problematic at room temperature. While it is broader at -196 ^{O}C (3.99 cm^{-1}), it is also only 0.48 cm^{-1} from the 1117 cm^{-1} Alanine band which is also considerably and would most certainly prevent its detection. Furthermore, the most dominant Histidine band at 1324 cm^{-1} is within 8.1 cm^{-1} of one of the two most dominant Glycine bands (1332 cm^{-1}). Both these bands are relatively wide and while the peak-to-valley ratio cannot be determined as it depends on the relative concentration and intensity, it is likely that a

resolution of at least 3-4 cm^{-1} will be necessary to fully resolve these two bands at -196 ^{O}C. As both of these bands are critical for the identification of Glycine and Histidine, the minimum spectral resolution for full identification is dictated by the proximity of these bands. Furthermore, a resolution of at least 2.74 cm^{-1} may be required to fully resolve the narrow Histidine 1117 cm^{-1} band.

The detection of a mixture of Alanine and Histidine may be even more restricted in terms of spectral resolution. At -196 ^{O}C, one of the most dominant bands in the spectra of Alanine (1315 cm^{-1}) lies within 9.39 cm^{-1} of the Histidine band 1324 cm^{-1}. Both are dominant and wide bands that could merge and become unresolvable if resolution greater than 9.39 cm^{-1} is not available, which would be critical for the identification of both Alanine and Histidine. Additionally, Alanine bands at 400 cm^{-1} and 533 cm^{-1}, which are also dominant Alanine bands and important for its identification, are within 2.67 cm^{-1} and 7.23 cm^{-1} of an adjacent Histidine band, respectively. Most importantly, one of the two most important Alanine bands at 855 cm^{-1} lies within only 2.02 cm^{-1} of a Histidine 857 cm^{-1} band. There are 6 Histidine bands within 3 cm^{-1} of an Alanine band including at least 3 that are important for the identification of Histidine (657 cm^{-1}, 857 cm^{-1} and 926 cm^{-1}). These 6 potentially unresolvable bands represent 18% and 27% of all detectable Raman bands of Histidine and Alanine respectively. Out of these Histidine 6 bands, 3 lie within 2 cm^{-1} of one another and 1 band within 1 cm^{-1}, however, this band is not a particularly important marker in either spectra. A

spectral resolution of <2.02 cm^{-1} may be able to resolve all except for 3 Histidine bands with only 2 bands being potentially important for identification. In this case the majority of the bands could be resolvable and used for confirmation. Nevertheless, a resolution better than 1.92 cm^{-1} may be necessary for full and unambiguous identification.

On the contrary, the resolution of the mixture of Histidine and Tryptophan does not seem to require a very high spectral resolution in comparison to the mixtures of other amino acids. There are 6 potentially unresolvable Histidine bands within 10 cm^{-1} of a Tryptophan band at -196 ^{O}C and none of these Histidine bands are essential for its identification. However, the 6 potentially unresolvable bands represent 18% of all Histidine bands detectable at -196 ^{O}C and 35% of Tryptophan bands. As such it may be desirable to employ a higher spectral resolution than 10 cm^{-1}. The only Tryptophan band that may be important for its identification and that lies within close proximity to a Histidine band is the 1365 cm^{-1} band located 11.24 cm^{-1} from the 1354 cm^{-1} Histidine band. While the Histidine 1354 cm^{-1} band is a relatively minor peak, both bands are also relatively wide and depending on the relative concentration of these two amino acids, a higher resolution may be necessary to resolve them. While the required resolution is impossible to determine exactly as it depends on the relative concentration and peak intensity, a resolution of 5 cm^{-1} should be capable of resolving these two bands in most cases and could also resolve all except for 3 other non-essential

bands of Histidine and Tryptophan. A spectral resolution of 7 cm^{-1} may also be sufficient with only 5 non-essential bands potentially unresolvable (which constitutes 29% of Tryptophan bands and 15% of Histidine bands).

For a mixture of all 4 amino acids, even a relatively high spectral resolution of 3 cm^{-1} would not be enough to resolve 11 Histidine bands including a number of bands important for the identification of the 4 amino acids. A spectral resolution of <2 cm^{-1} would not be able to resolve only 6 Histidine bands (18%), however, this includes 2 bands potentially important for its identification. Similar to the resolution required for the identification of the mixture of Alanine and Histidine, a resolution better than 1.92 cm^{-1} could be sufficient to resolve all but 4 bands with only 1 being potentially important.

In comparison, SHERLOC, a miniaturised Raman Instrument developed for in-situ exploration of Mars that was launched on the Mars 2020 mission on the Perseverance rover, has a spectral resolution of 49 cm^{-1} (L. W. Beegle et al., 2020; Bhartia et al., 2021). As shown in the data in Table 2, it is important to note that the spectral resolution required based on the clearance between individual bands does not necessarily increase with decreasing temperature as some bands can shift further away from adjacent bands. This is also reflected in Table 3 which shows that while some peaks in a mixture of amino acids may shift closer and the number of potentially unresolvable bands at a certain resolution may thus increase

at -196 ^{O}C compared to room temperature, a higher spectral resolution may not be required. On the contrary, a lower spectral resolution may be sufficient in some cases as some bands may not be essential for the identification of the amino acids and some dominant bands important for identification may shift further apart from possible interferants at extreme low temperatures.

Another effect observed in the spectra that could severely impact the effectiveness of Raman spectroscopy for life detection on Europa is Raman band narrowing at extreme low temperatures. Except for some discrepancies in the spectra of Tryptophan, likely caused by the presence of fluorescence in the spectra, all Raman bands within all amino acid spectra obtained in this study showed a decreasing Raman band width with decreasing temperature. This is caused by the damping of the scattered light in the extreme cold environment. As shown in Figure 18 (b), similarly to the Raman shift change, this relationship could also be described by a 3rd order polynomial curve that would eventually converge to a flat line towards 0 K.

Table 2 shows the narrowest band width that was measured for spectra of the amino acids in this study at the temperatures 22 ^{O}C, -100 ^{O}C and -196 ^{O}C. Between 22 ^{O}C and -196 ^{O}C the most significant change in the Raman band width was a decrease of 24.67 cm^{-1} which is 80.1% of the nominal room temperature width and was recorded in the spectra of Glycine. The minimum band width

change was 0.87 cm^{-1} (12.7%) or 4.4% in percentage (1.03 cm^{-1}) detected in the spectra of Tryptophan and Histidine respectively. Similar to the Raman shift change, this is specific to a particular molecule and a molecular bond. However, the data suggests that at temperatures analogous to Europa, amino acid Raman bands could narrow by as much as 80.1%. This represents a significant spectral change and could greatly affect the detectability of some molecules at extreme low temperatures analogous to Europa and the analysis of spectra obtained at these conditions. The narrower Raman bands might prove problematic for detection as a higher spectral resolution is needed. This is a particular concern for Raman spectroscopy for Europa and other extraterrestrial applications. Miniaturised Raman instruments tend to have lower spectral resolution as a result of the mass and size trade off that is necessary in order to comply with the strict design constraints for extraterrestrial exploration.

The spectral resolution for an instrument aiming to fully detect Glycine, Alanine, Histidine or Tryptophan will need to be better than the values recorded in Table 2 and Table 3. For a Raman instrument operating on Europa at -196 ^{O}C and aiming to detect Histidine, which is an important biosignature for the detection of extraterrestrial life, the minimum spectral resolution could be as high as 2.02 cm^{-1}, which could be a challenge for miniaturised Raman instruments. There are currently two Raman instruments for planetary exploration that have been launched to date, SHERLOC and SuperCam (both launched on the Mars 2020

Mission)(Farley et al., 2020). As already discussed above, SHERLOC's deep UV excitation design is limited to the spectral resolution of 49 cm^{-1} and SuperCam has a spectral resolution of 12 cm^{-1} (L. W. Beegle et al., 2020; Farley et al., 2020). Based on data collected in this study and as summarized in Table 2 and Table 3, this will not be sufficient to fully resolve the spectra of Glycine, Alanine, Histidine and Tryptophan and might be particularly problematic for the detection of Histidine. While concepts and prototypes of miniaturized instruments for planetary exploration with a better spectral resolution exist, none have space heritage to date and most do not meet the spectral resolution outlined in this study, particularly for the detection of amino acids in mixtures (Blacksberg et al., 2016; J. L. Lambert, 2018, 2020; Lamsal & Angel, 2015; Wang et al., 2003).

At the same time, as evident in the spectra obtained and shown in Figure 1, Figure 5, Figure 9 and Figure 13, the narrower bands might allow easier resolution of individual Raman bands at lower temperatures. Adversely, this could lead to a lower spectral resolution requirement for Raman instruments operating at extreme low temperatures. The narrower Raman bands at extreme low temperatures also offer higher precision measurements, which might be particularly useful in a mixture of compounds and for studies of material properties. Such an advantage might be beneficial for a much wider range of applications than extraterrestrial exploration and the detection of biosignatures on Europa.

The higher precision of Raman measurements at extreme low temperatures is also supported by the Raman shift and width variance data. All amino acids analysed in this study show a decrease in the average variance of the spectra between individual measurements at extreme low temperatures. This could be assigned to the molecular bonding and vibrations being more constrained at lower temperatures. The variance dependence on temperature appears linear for the Raman shift data and drops from the highest room temperature average variance of 0.157% (Glycine) to the highest average variance of 0.066% (Tryptophan) at -196 ^{O}C. While the Raman band width variance decrease towards lower temperatures proved to be less consistent than the Raman shift variance, a decreasing trend was observed in the spectra of all amino acids. The highest band width variance at room temperature across all amino acids was 17.7% (Tryptophan) and the highest variance at -196 ^{O}C was 16% (Tryptophan). The discrepancies in the band width variance data are attributed to the dependence of Raman band width readings on changes within molecular bonds and other material or environmental disturbances such as the presence of a fluorescent background.

The decreasing variance at extreme low temperatures leads to higher precision Raman measurements, which could be beneficial for a mission to Europa where the sampled material is of unknown composition and might contain a variety of compounds with interfering Raman spectra. As mentioned above, other

applications could also benefit from the higher definition offered by low temperature Raman spectroscopy.

The emergence of new Raman bands at low temperatures was recorded in the spectra of Glycine, Alanine and Histidine either due to enhanced definition as a result of narrower and higher intensity Raman bands or due to the shifting of Raman bands to higher or lower frequencies and splitting from an adjacent band. These additional data points only resolvable at extreme low temperatures could allow a more complete analysis of the studied material and provide more information about its composition and material properties. However, in some cases it could also increase the spectral resolution requirement. Particularly, two new bands previously undetectable at room temperature appear at -100 ^{O}C in the region between 300 cm^{-1} to 440 cm^{-1} in the spectra of Histidine. This results in 5 Raman bands closely packed in this region at extreme low temperatures rather than 3 at room temperature possibly causing discrepancies in Raman shift readings as the bands blend together in the spectra if the spectral resolution is insufficient. As mentioned above, this higher spectral resolution requirement might be challenging for miniaturised Raman instruments for in-situ space exploration and it may result in limited data output.

The diminishing of Raman bands at lower temperatures was also recorded in the spectra of Histidine and Alanine. This was mostly due to loss of intensity at lower

temperatures as well as the Raman bands shifting towards adjacent bands and blending together. While the emerging peaks resulted in relatively minor changes in the spectra of the examined amino acids, in general the emergence and diminishing of Raman bands at extreme low temperatures could deem Raman spectra obtained on Earth and at room temperatures unrepresentative of the spectra potentially obtained on Europa or other Icy Worlds.

Significant changes in the signal intensity occurred in the spectra of all examined amino acids. However, the changes are specific to individual Raman bands rather than a uniform change across the entire spectrum. Overall, all fully detectable Glycine bands increased in intensity at -196 ^{O}C compared to that at 22 ^{O}C and the overall trend in intensity change across Histidine bands also suggests an intensity increase at extreme low temperatures. On the contrary, the signal intensity of all the fully detectable Alanine Raman bands decreased at extreme low temperatures and there was an equal distribution of bands with increasing and decreasing intensity in the spectra of Tryptophan.

Across the examined amino acids the maximum signal increase observed between room temperature and -196 ^{O}C was 37% and the maximum decrease was 67.8%. While this could be specific to the Raman bands and spectra of the amino acids examined in this study, it could provide a general indication that the intensity of individual Raman bands at -196 ^{O}C on Europa could be as high as a 37% decrease

or 67.8% increase. While the signal intensity data can be easily affected by experimental disturbances and may not be conclusive, the data collected also suggests that there is no clear common pattern in intensity changes induced by extreme low temperatures in the spectra of the examined amino acids.

A potentially detrimental effect for the detection of biosignatures on Europa observed at extreme low temperatures is the increase in the fluorescence background. This effect was only observed in the spectra of Tryptophan, as among the examined amino acids only Tryptophan fluoresces at 785 nm excitation at room temperature. While this only applies to molecules which fluoresce at room temperature at a certain excitation, most biosignatures fluoresce at excitations commonly used in Raman spectroscopy such as 532 nm and 633 nm. While most traditional biosignatures such as amino acids and nucleobases can be detected using 785 nm excitation without any fluorescent background in the spectra, there are exceptions such as Tryptophan and Adenine that do fluoresce mildly at this excitation. Other important biomarkers for astrobiology could also fluoresce at 785 nm excitation and the increase in fluorescence could greatly affect their detectability.

As shown in the S/N ratio analysis in Figure 14, the recorded rise in fluorescent background at decreasing temperature in the Tryptophan spectra appears linear with a 0.2786 K^{-1} rate of change. This rise in fluorescence can be assigned to the

reduction of radiationless decay and extra energy heat loss due to collisions, as the lower temperatures impede the movement of molecules decreasing the transitional energy and thus reducing the number of collisions.

The rise in the fluorescent background could be particularly problematic for a mixture of compounds including fluorescing molecules which could then overshadow the spectra of other molecules in the mixture. Without prior sample manipulation, a sample collected on Europa would inherently contain a mixture of compounds, some of which may be fluorescent. A successful detection of target molecules might thus require additional procedures or instrument design modifications, such as time-gating or the application of multiple excitation wavelengths, surface enhanced Raman spectroscopy and fluorescence reduction computational methods, in order to reduce the effects of the fluorescent background.

An analysis of other fluorescent molecules important to astrobiology or specific to the composition of the Europan icy shell at extreme low temperatures is necessary to confirm the observed trends and the full impact of the increased fluorescence on life detection on Europa.

Most of the effects observed in the spectra of the examined amino acids at extreme low temperatures are molecule specific and could have a significant impact on the detectability of molecules on Europa. Further research is necessary

to confirm the trends and changes in the spectra of other molecules important for astrobiology at temperatures analogous to Icy Worlds, such as Europa, Enceladus or Titan, in order to inform the design of potential Raman instruments and ensure successful detection of the target molecules. A detailed review of the spectra of biomarkers for extraterrestrial exploration at extreme low temperatures could also assist with the analysis of the data collected during any future missions.

5. Conclusions

Raman spectra of amino acids representing important biosignatures for the search for life on Europa, Glycine, Alanine, Histidine and Tryptophan, were presented and analysed at 22 ^{O}C, -100 ^{O}C and -196^{O}C. The effects of the extreme low temperatures on the spectra were recorded and quantified. The results indicate that these extreme low temperatures analogous to Europa could have significant impact on the Raman spectra of target molecules for the search for Europan life.

Spectral changes induced by the extreme low temperatures include shifting of Raman bands to higher or lower frequencies, narrowing of the Raman band width, decrease in the variance between individual spectra, the emergence of new bands or the diminishing of existing Raman bands as well as changes in the signal intensity and increasing fluorescence background. Changes common for all examined amino acids and most of the Raman bands within their spectra are

shifting of Raman bands to higher frequencies and narrowing of the band width. Other observed changes were more specific to a particular molecule and Raman band.

The results clearly indicate that there is a link between the type of the vibrational mode associated with Raman bands and the change in their Raman shift at extreme low temperatures. Specifically, bands associated with vibrations relatively constrained within the structure of the molecule, that is, stretching vibrational modes, out of plane deformation of a ring or vibrations including inner atoms of a molecule, are more likely to shift to lower frequencies at low temperatures or shift to higher frequencies only by a small amount compared to bands assigned to other vibrational modes. On the contrary, bands that shift to a significantly higher frequency at lower temperature tend to be exclusively associated at least partially with vibrational modes including the outer parts of a molecule, such as its side chains, outer atoms and groups, or vibrations including most or all of the molecule main chain or in plane bending within a ring, which are vibrations that are relatively less constrained within the molecular structure.

The observed shifting of the Raman bands, as well as the narrowing of Raman band width and emergence of new bands in the Raman spectra at extreme low temperatures, affect the instrument design requirements for a mission to Europa as higher spectral resolution may be necessary for the successful identification of

molecules. The spectral resolution necessary to fully resolve the amino acids examined in this study at a temperature analogous to Europa of -196 ^{O}C could be as high as 2 cm^{-1} or higher depending on the mixture of molecules in the sample.

However, thanks to the Raman band narrowing and decreased spectral variance at extreme low temperatures Raman Spectroscopy can also offer higher definition spectra at extreme low temperatures which could also be an advantage for the exploration of Europa and other Icy Worlds.

The linearly increasing fluorescence background detected in the spectra of Tryptophan suggests that extreme low temperatures may have a significant impact on the detectability of some biosignatures important for astrobiology or target molecules in a mixture of compounds containing fluorescent molecules. This might require an instrument design incorporating fluorescence reduction techniques such as time-gating, surface enhancement, or computational methods to ensure successful detection of target molecules.

As shown in the results, the changes in the Raman spectra at extreme low temperatures are molecule specific and could be a driving factor in the instrument design. As such, a full detailed review of biosignatures and other target molecules relevant for the search for life on Europa is necessary to inform the design of potential life detecting Raman instruments for a mission to Europa and ensure successful detection.

6. Acknowledgements

We would like to thank the University of Southampton and the Astronautics Department for providing the resources to carry out this research as well as laboratory technicians, Mike Bartlett and Jon Kerly, for assisting with the supply of liquid nitrogen for the experiments.

7. Authorship Confirmation Statement

All authors, including the co-authors, are responsible for a significant part of the manuscript and have taken part in writing the manuscript, reviewing it, and revising its intellectual and technical content. All persons who meet authorship criteria are listed as authors, and all authors certify that they have participated sufficiently in the work to take public responsibility for the content, including participation in the concept, design, analysis, writing, review or revision of the manuscript. Furthermore, each author certifies that this material or similar material has not been and will not be submitted to or published in any other publication before its appearance in the Astrobiology Journal.

8. Author Disclosure Statement

No competing financial interests exist.

9. Funding Statement

There is no funding information to declare.

10. References

Abbey, W. J., Bhartia, R., Beegle, L. W., Deflores, L., Paez, V., Sijapati, K., Sijapati, S., Williford, K., Tuite, M., Hug, W., & Reid, R. (2017). Deep UV Raman spectroscopy for planetary exploration: The search for in situ organics. *Icarus*, *290*, 201–214. https://doi.org/10.1016/j.icarus.2017.01.039

Anderson, J. D., Lau, E. L., Sjogren, W. L., Schubert, G., & Moore, W. B. (1997). Europa´s Differentiated Internal Structure: Inferences from Two Galileo Encounters. *Science*, *276*(5316), 1236–1239. https://doi.org/10.1126/science.276.5316.1236

Ashkenazy, Y. (2016). *The surface temperature of Europa*.

Beegle, L., Bhartia, R., White, M., Deflores, L., Abbey, W., Wu, Y. H., Cameron, B., Moore, J., Fries, M., Burton, A., Edgett, K. S., Ravine, M. A., Hug, W., Reid, R., Nelson, T., Clegg, S., Wiens, R., Asher, S., & Sobron, P. (2015). SHERLOC: Scanning habitable environments with Raman & luminescence for organics & chemicals. *IEEE Aerospace Conference Proceedings*.

https://doi.org/10.1109/AERO.2015.7119105

Beegle, L. W., Bhartia, R., DeFlores, L., Abbey, W., Miller, E., Bailey, Z., Hollis, J. R., Pollack, R., Asher, S., Burton, A., Fries, M., Conrad, P., Clegg, S., Edgett, K. S., Ehlmann, B., Hug, W., Reid, R., Kah, L., Nealson, K., … Yingst, R. A. (2020). The SHERLOC Investigation on the Mars 2020 Rover. *51st Lunar and Planetary Science Conference*.

Berg, R. W. (2018). Raman detection of hydrohalite formation: Avoiding accidents on icy roads by deicing where salt will not work. *Applied Spectroscopy Reviews*, *53*(6), 503–515. https://doi.org/10.1080/05704928.2017.1396540

Bhartia, R., Beegle, L. W., DeFlores, L., Abbey, W., Razzell Hollis, J., Uckert, K., Monacelli, B., Edgett, K. S., Kennedy, M. R., Sylvia, M., Aldrich, D., Anderson, M., Asher, S. A., Bailey, Z., Boyd, K., Burton, A. S., Caffrey, M., Calaway, M. J., Calvet, R., … Zan, J. (2021). Perseverance's Scanning Habitable Environments with Raman and Luminescence for Organics and Chemicals (SHERLOC) Investigation. In *Space Science Reviews* (Vol. 217). The Author(s). https://doi.org/10.1007/s11214-021-00812-z

Blacksberg, J., Alerstam, E., Maruyama, Y., Cochrane, C. J., & Rossman, G. R. (2016). Miniaturized time-resolved Raman spectrometer for planetary

science based on a fast single photon avalanche diode detector array. *Applied Optics*, *55*(4), 739. https://doi.org/10.1364/AO.55.000739

Chuang, C. H., & Chen, Y. T. (2009). Raman scattering of L-tryptophan enhanced by surface plasmon of silver nanoparticles: Vibrational assignment and structural determination. *Journal of Raman Spectroscopy*, *40*(2), 150–156. https://doi.org/10.1002/jrs.2097

Chyba, C. F., & Phillips, C. B. (2001). Possible ecosystems and the search for life on Europa. *Proceedings of the National Academy of Sciences*, *98*(3), 801–804. https://doi.org/10.1073/PNAS.98.3.801

Clegg, S. M., Wiens, R., Misra, A. K., Sharma, S. K., Lambert, J., Bender, S., Newell, R., Nowak-Lovato, K., Smrekar, S., Dyar, M. D., & Maurice, S. (2015). Planetary geochemical investigations using raman and laser-induced breakdown spectroscopy. *Applied Spectroscopy*, *68*(9), 925–936. https://doi.org/10.1366/13-07386

Committee on the Planetary Science Decadal Survey. (2011). *Vision and Voyages for Planetary Science in the Decade 2013-2022*. The National Academies Press.

Creamer, J. S., Mora, M. F., & Willis, P. A. (2017). Enhanced Resolution of Chiral Amino Acids with Capillary Electrophoresis for Biosignature

Detection in Extraterrestrial Samples. *Analytical Chemistry*, *89*(2), 1329–1337. https://doi.org/10.1021/acs.analchem.6b04338

Deckert-Gaudig, T., & Deckert, V. (2009). Tip-enhanced Raman scattering studies of histidine on novel silver substrates. *Journal of Raman Spectroscopy*, *40*(10), 1446–1451. https://doi.org/10.1002/jrs.2359

Farley, K. A., Williford, K. H., Stack, K. M., Bhartia, R., Chen, A., de la Torre, M., Hand, K., Goreva, Y., Herd, C. D. K., Hueso, R., Liu, Y., Maki, J. N., Martinez, G., Moeller, R. C., Nelessen, A., Newman, C. E., Nunes, D., Ponce, A., Spanovich, N., … Wiens, R. C. (2020). Mars 2020 Mission Overview. *Space Science Reviews*, *216*, 142. https://doi.org/10.1007/s11214-020-00762-y

Freire, P. T. C., Barboza, F. M., Lima, J. A., Melo, F. E. A., & Filho, J. M. (2017). Raman Spectroscopy of Amino Acid Crystals. In *Raman Spectroscopy and Applications*. INTECH. https://doi.org/10.5772/65480

Fretwell, P., Pritchard, H. D., Vaughan, D. G., Bamber, J. L., Barrand, N. E., Bell, R., Bianchi, C., Bingham, R. G., Blankenship, D. D., Casassa, G., Catania, G., Callens, D., Conway, H., Cook, A. J., Corr, H. F. J., Damaske, D., Damm, V., Ferraccioli, F., Forsberg, R., … Zirizzotti, A. (2013). Bedmap2: Improved ice bed, surface and thickness datasets for Antarctica. *Cryosphere*,

7(1), 375–393. https://doi.org/10.5194/tc-7-375-2013

Fukushima, K., Onishi, T., Shimanouchi, T., & Mizushima, S. ichiro. (1959). Assignment of vibration bands of DL-alanine. *Spectrochimica Acta*, *15*, 236–241. https://doi.org/10.1016/s0371-1951(59)80312-x

Gasda, P. J., Wiens, R. C., Misra, A. K., Acosta-Maeda, T. E., Sharma, S. K., Quinn, H., Ganguly, K., Newell, R. T., Clegg, S., Maurice, S., Virmontois, C., Love, S. P., Nelson, T., Ott, L., & Sandoval, B. (2021). OrganiCam: A Time-Resolved Fluorescence Imager and Raman Spectrometer for Organic Reconnaissance. *2021 Virtual In Situ Science and Instrumentation Workshop for the Exploration of Europa and Ocean Worlds*.

Girardot, C., Kreisel, J., Pignard, S., Caillault, N., & Weiss, F. (2008). Raman scattering investigation across the magnetic and metal-insulator transition in rare earth nickelate R NiO3 (R=Sm, Nd) thin films. *Physical Review B - Condensed Matter and Materials Physics*, *78*(10). https://doi.org/10.1103/PhysRevB.78.104101

Haines, J., Rouquette, J., Bornand, V., Pintard, M., Papet, P., & Gorelli, F. A. (2003). Raman scattering studies at high pressure and low temperature: Technique and application to the piezoelectric material Pbzr0.52Ti 0.48O3. *Journal of Raman Spectroscopy*, *34*(7–8), 519–523.

https://doi.org/10.1002/jrs.1009

Hand, K. P., Murray, A. ., Gavin, J. B., Brickerhoff, W. B., Christner, B. C., Edgett, K. S., Ehlmann, B. L., German, C. R., Hayes, A. G., Hoehler, T. M., Horst, S. M., Lunine, J. I., Nealson, K. H., Paranicas, C., Schmidt, B. E., Smith, D. E., Rhoden, A. R., Russell, M. J., Templeton, A. S., … and the Project Engineering Team (2017). (2017). *Europa Lander Mission - Europa Lander Study 2016 Report*. Jet Propulsion Laboratory, NASA.

Hibbert, R., Price, M. C., Kinnear, T. M., Cole, M. J., & Burchell, M. J. (2015). The effects of temperature on the Raman spectrum of high purity quartz crystals. *46th Lunar and Planetary Science Conference*.

Hiscox, J. A. (2000). Outer solar system, Europa, Titan and the possibility of life. In *Astronomy & Geophysics* (Vol. 41, Issue 5). https://doi.org/10.1046/j.1468-4004.2000.41523.x

Jalkanen, K. J., Nieminen, R. M., Frimand, K., Bohr, J., Bohr, H., Wade, R. C., Tajkhorshid, E., & Suhai, S. (2001). A comparison of aqueous solvent models used in the calculation of the Raman and ROA spectra of L-alanine. *Chemical Physics, 265*, 125–151. https://doi.org/10.1016/S0301-0104(01)00267-1

Jehlicka, J., Edwards, H. G. M., & Culka, A. (2010). Using portable Raman

spectrometers for the identification of organic compounds at low temperatures and high altitudes: Exobiological applications. *Philosophical Transactions of the Royal Society A: Mathematical, Physical and Engineering Sciences*, *368*(1922), 3109–3125. https://doi.org/10.1098/rsta.2010.0075

Krajewski, J., Hand, K., Gibbs, R., Doodley, J., Tan-Wang, G., & Danesh, P. (2018). *Europa Lander Science Payload - Draft Proposal Information Package*. Jet Propulsion Laboratory, NASA.

Kumar, S., Kumar Rai, A., Rai, S. B., Rai, D. K., Singh, A. N., & Singh, V. B. (2006). Infrared, Raman and electronic spectra of alanine: A comparison with ab intio calculation. *Journal of Molecular Structure*, *791*, 23–29. https://doi.org/10.1016/j.molstruc.2006.01.004

Kumar, S., Rai, A. K., Rai, S. B., & Rai, D. K. (2010). Infrared and Raman spectra of Histidine: an ab initio DFT calculations of Histidine molecule and its different protonated forms. *Indian Journal of Physics*, *84*(5), 563–573.

Lambert, J. L. (2018). *Context imaging raman spectrometer* (Patent No. US Patent 10,048,130 B2).

Lambert, J. L. (2020). *Dual Wavelength Context Imaging Raman and*

Fluorescence Spectrometer (Patent No. US Patent 10,746,600 B2).

Lambert, J., & Wang, A. (2019). Overview of the Compact Integrated Raman Spectrometer (CIRS) for an Europa Lander Mission. *Astrobiology Science Conference, AGU*.

Lamsal, N., & Angel, S. M. (2015). Deep-ultraviolet Raman measurements using a spatial heterodyne Raman spectrometer (SHRS). *Applied Spectroscopy*, *69*(5), 525–534. https://doi.org/10.1366/14-07844

Le Tacon, M., Sacuto, A., Georges, A., Kotliar, G., Gallais, Y., Colson, D., & Forget, A. (2006). Two energy scales and two distinct quasiparticle dynamics in the superconducting state of underdoped cuprates. *Nature Physics*, *2*(8), 537–543. https://doi.org/10.1038/nphys362

Liljeblad, J. F. D., Furó, I., & Tyrode, E. C. (2017). The premolten layer of ice next to a hydrophilic solid surface: correlating adhesion with molecular properties. *Physical Chemistry Chemical Physics*, *19*(1), 305–317. https://doi.org/10.1039/c6cp05303c

Martusevičius, S., Niaura, G., Talaikyte, Z., & Razumas, V. (1996). Adsorption of L-histidine on copper surface as evidenced by surface-enhanced Raman scattering spectroscopy. *Vibrational Spectroscopy*, *10*(2), 271–280.

https://doi.org/10.1016/0924-2031(95)00025-9

Mesu, J. G., Visser, T., Soulimani, F., & Weckhuysen, B. M. (2005). Infrared and Raman spectroscopic study of pH-induced structural changes of L-histidine in aqueous environment. *Vibrational Spectroscopy*, *39*(1), 114–125. https://doi.org/10.1016/j.vibspec.2005.01.003

Nimmo, F., & Manga, M. (2004). Geodynamics of Europa's Icy Shell. In K. K. K. Robert T. Pappalardo, William B. McKinnon (Ed.), *Europa* (pp. 381–404).

Nordheim, T. A., Hand, K. P., & Paranicas, C. (2018). Preservation of potential biosignatures in the shallow subsurface of Europa. *Nature Astronomy*, *2*, 673–679.

Pershin, S. M., Lednev, V. N., Yulmetov, R. N., Klinkov, V. K., & Bunkin, A. F. (2015). Transparent material thickness measurements by Raman scattering. *Applied Optics*, *54*(19), 5943. https://doi.org/10.1364/ao.54.005943

Phillips-Lander, C. M., Moore, T. Z., Raut, U., Molyneux, P. M., Miller, M. A., Nowicki, K., Blase, R. C., Davis, M. W., Veach, T. J., Dirks, G. J., Persson, K. B., Tyler, Y. D., Klar, R. A., Karnes, P. L., Freeman, M. A., Howett, J. A., Soto, A., Mandt, K., Roth, L., … Retherford, K. (2019). Europa Integrating Cavity Enhanced Raman Spectroscometer for Exploration of Icy Worlds (ERSO) Concept. *50th Lunar and Planetary Science Conference*

2019, 2132.

Prieto-Ballesteros, O., Vorobyova, E., Parro, V., Rodriguez Manfredi, J. A., & Gó Mez, F. (2011). Strategies for detection of putative life on Europa. *Advances in Space Research*, *48*, 678–688. https://doi.org/10.1016/j.asr.2010.11.010

Rodriguez-Manfredi, J. A., Prieto-Ballesteros, O., Gomez, F., & Sansano, A. (n.d.). *Raman spectrometer for in-situ measurements on Europa's surface*.

Rolfe, S. M., Patel, M. R., Gilmour, I., Olsson-Francis, K., & Ringrose, T. J. (2016). Defining Multiple Characteristic Raman Bands of α-Amino Acids as Biomarkers for Planetary Missions Using a Statistical Method. *Origins of Life and Evolution of Biospheres*, *46*, 323–346. https://doi.org/10.1007/s11084-015-9477-7

Rosado, M. T., Duarte, M. L. T. S., & Fausto, R. (1998). Vibrational spectra of acid and alkaline glycine salts. *Vibrational Spectroscopy*, *16*, 35–54. https://doi.org/10.1016/S0924-2031(97)00050-7

Rosado, M. T. S., Duarte, M. L. R. S., & Fausto, R. (1997). Vibrational spectra (FT-IR, Raman and MI-IR) of α- and β-alanine. *Journal of Molecular Structure*, *410–411*, 343–348. https://doi.org/10.1016/S0022-2860(96)09695-0

Rull, F., Maurice, S., Hutchinson, I., Moral, A., Perez, C., Diaz, C., Colombo, M.,

Belenguer, T., Lopez-Reyes, G., Sansano, A., Forni, O., Parot, Y., Striebig, N., Woodward, S., Howe, C., Tarcea, N., Rodriguez, P., Seoane, L., Santiago, A., … Vago, J. L. (2017). The Raman Laser Spectrometer for the ExoMars Rover Mission to Mars. *Astrobiology*, *17*(6 and 7), 627–654. https://doi.org/10.1089/ast.2016.1567

Sandilands, L. J., Tian, Y., Plumb, K. W., Kim, Y. J., & Burch, K. S. (2015). Scattering Continuum and Possible Fractionalized Excitations in α-RuCl3. *Physical Review Letters*, *114*(14), 1–7. https://doi.org/10.1103/PhysRevLett.114.147201

Scambos, T. A., Campbell, G. G., Pope, A., Haran, T., Muto, A., Lazzara, M., Reijmer, C. H., & van den Broeke, M. R. (2018). Ultralow Surface Temperatures in East Antarctica From Satellite Thermal Infrared Mapping: The Coldest Places on Earth. *Geophysical Research Letters*, *45*(12), 6124–6133. https://doi.org/10.1029/2018GL078133

Sobron, P., & Wang, A. (2011). Low-temperature Raman Spectroscopy of Materials Relevant for Planetary Exploration. *42nd Lunar and Planetary Science Conference*.

Stenback, H. (1976). On the Raman spectra of solid natural alpha-glycine and solid 15N-substituted alpha-glycine. *Journal of Raman Spectroscopy*, *5*, 49–

55.

Sutherland, G. B. B. M. (1933). Experiments on the raman effect at very low temperatures. *Proceedings of the Royal Society of London A: Mathematical and Physical and Engineering Sciences*, *141*(845), 535–549. https://doi.org/10.1098/rspa.1933.0137

Tajkhorshid, E., Jalkanen, K. J., & Suhai, S. (1998). Structure and Vibrational Spectra of the Zwitterion L-Alanine in the Presence of Explicit Water Molecules: A Density Functional Analysis. *Journal of Physical Chemistry B*, *102*(30), 5899–5913. https://doi.org/10.1016/S0022-2860(02)00680-4

Tarcea, N., Harz, M., Rösch, P., Frosch, T., Schmitt, M., Thiele, H., Hochleitner, R., & Popp, J. (2007). UV Raman spectroscopy-A technique for biological and mineralogical in situ planetary studies. *Spectrochimica Acta - Part A: Molecular and Biomolecular Spectroscopy*, *68*(4), 1029–1035. https://doi.org/10.1016/j.saa.2007.06.051

Tobie, G., Choblet, G., & Sotin, C. (2003). Tidally heated convection : Constraints on Europa ' s ice shell thickness. *Joural of Geophysical Research*, *108*, 1–15. https://doi.org/10.1029/2003JE002099

Wang, A., Haskin, L. A., Lane, A. L., Wdowiak, T. J., Squyres, S. S., Wilson, R. J., Hovland, L. E., Manatt, K. S., Raouf, N., & Smith, C. D. (2003).

Development of the Mars microbeam Raman spectrometer (MMRS). *Journal of Geophysical Research E: Planets*, *108*(E1), 5005. https://doi.org/10.1029/2002je001902

Weber, I., Böttger, U., Pavlov, S. G., Jessberger, E. K., & Hübers, H. W. (2014). Mineralogical and Raman spectroscopy studies of natural olivines exposed to different planetary environments. *Planetary and Space Science*, *104*, 163–172. https://doi.org/10.1016/j.pss.2014.08.016

Zhu, G., Zhu, X., Fan, Q., & Wan, X. (2011). Raman spectra of amino acids and their aqueous solutions. *Spectrochimica Acta - Part A: Molecular and Biomolecular Spectroscopy*, *78*(3), 1187–1195. https://doi.org/10.1016/j.saa.2010.12.079

Zolotov, M., Shock, E. L., & Zolotov, M. Y. (2004). A model for low-temperature biogeochemistry of sulfur, carbon, and iron on Europa. *Journal of*

Geophysical Research, 109, 6003. https://doi.org/10.1029/2003JE002194

11. Correspondence Address

Hanna Sykulska-Lawrence

Affiliation: Astronautics Research Group, University of Southampton

Mailing Address: University of Southampton, Southampton, SO17 1BJ, UK

(office: B176/2033)

Phone: +44(0)2380 592313

E-mail: H.M.Sykulska-Lawrence@soton.ac.uk

12. Figure Legends

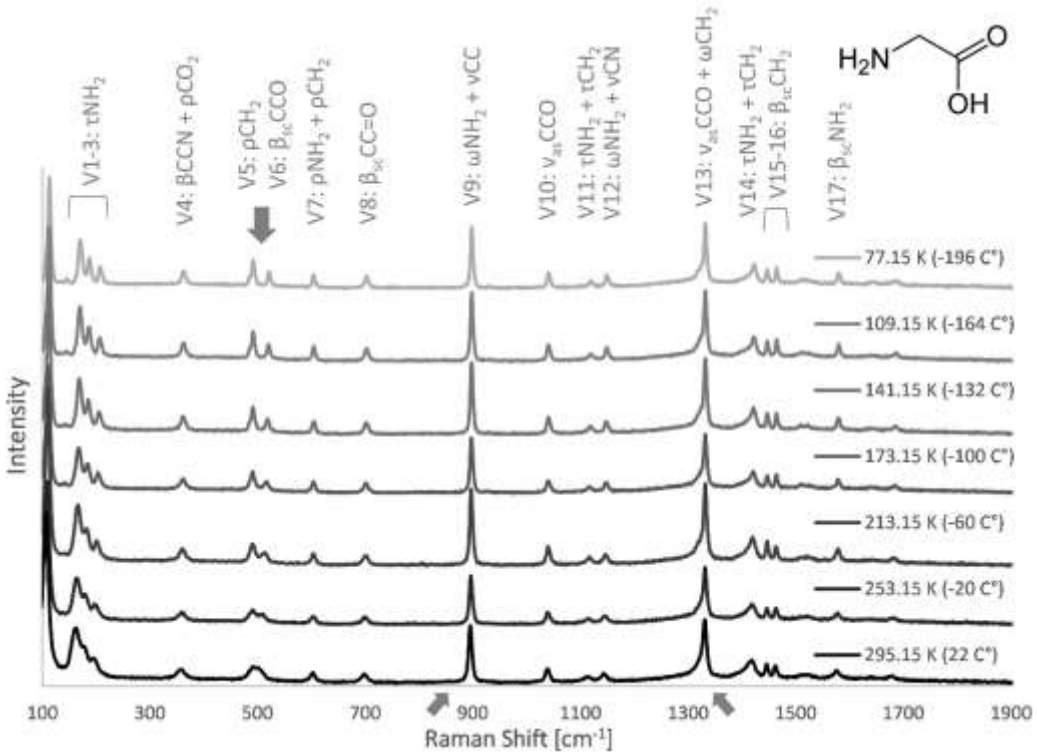

Figure 1 Raman spectra of Glycine at various temperatures in the range of 22 ^{O}C to -196 ^{O}C, where ν = stretching, ω = wagging, ρ = rocking, β = bending, τ = torsion, sc = scissoring, as = asymmetric. Assignments are based on an optimized Density Functional Theory (DFT) vibrational frequency calculation using Split Valence Polarization (SVP) and polarizability calculations for Raman vibrational frequencies and Raman activity together with a review of previously published assignments (Rolfe et al., 2016; M. T. Rosado et al., 1998; Stenback, 1976). A

vertical arrow highlights the split of the 497 cm^{-1} band, diagonal arrows highlight bands detailed in Figure 2.

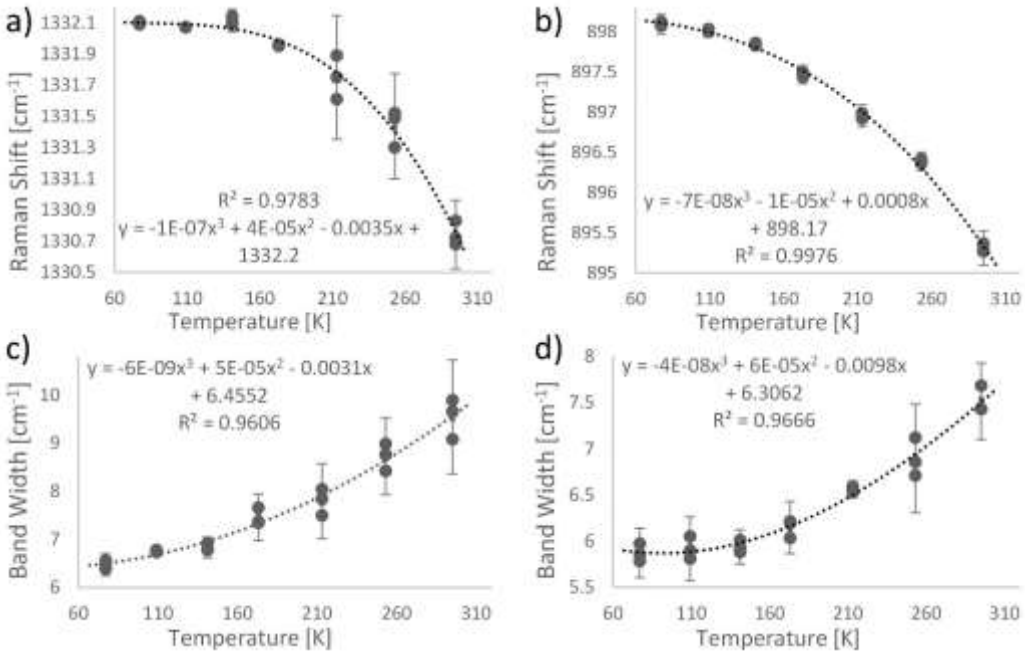

Figure 2 The profile of the changes in the Raman band shift and width of the Glycine asymmetrical stretching of CCO Raman band at 1331 cm^{-1} (a and c respectively) and NH_2 wagging at 895 cm^{-1} (b and d respectively). These bands are highlighted with arrows in the spectra in Figure 1. A general trend of the change is highlighted using a 3rd order polynomial curve. 2σ error bars calculated for these peaks at each temperature over 3 measurements at 3 different power settings are included in (a), (c) and (d) to indicate the relative significance of the changes. 3σ error bars are displayed in (b) as the change was too great for 2σ error bars to be visible.

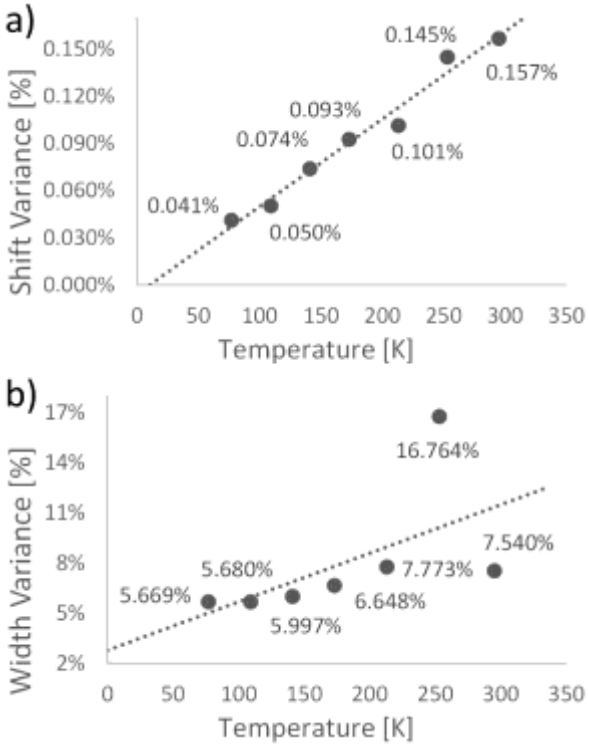

Figure 3 Variance of Raman band shift (a) and width (b) across individual Glycine spectra as a function of temperature

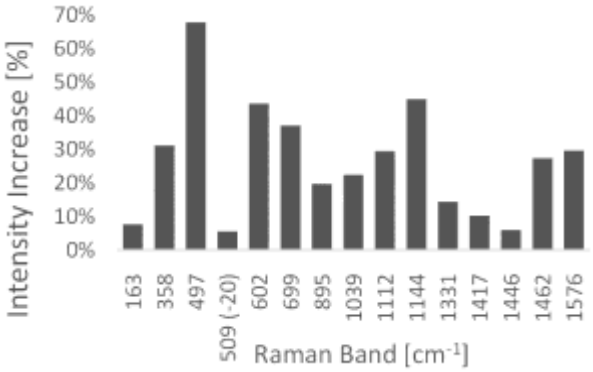

Figure 4 Intensity increase of Glycine Raman spectra at 196 ^{O}C compared to room temperature measurements

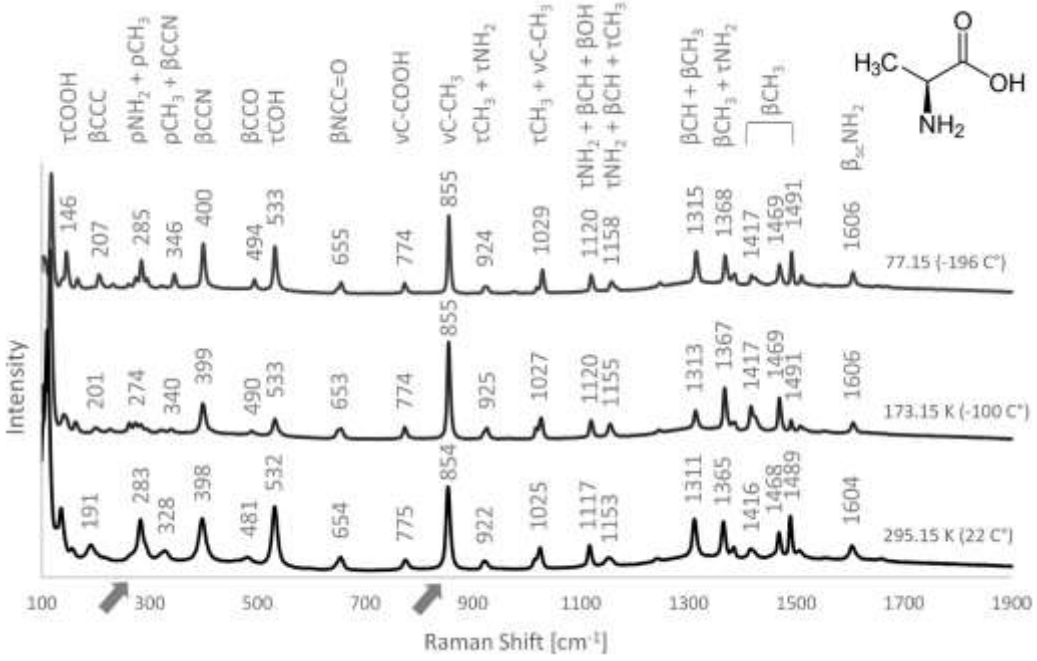

Figure 5 Raman spectra of Alanine at 22 ^{O}C, -100 ^{O}C and -196 ^{O}C, where ν = stretching, β = bending, τ = torsion, sc = scissoring. Assignments are based on an optimized DFT vibrational frequency calculation using SVP and polarizability

calculations for Raman vibrational frequencies and Raman activity together with a review of previously published assignments (Freire et al., 2017; Fukushima et al., 1959; Jalkanen et al., 2001; Kumar et al., 2006; Rolfe et al., 2016; M. T. S. Rosado et al., 1997; Tajkhorshid et al., 1998). Arrows highlight bands detailed in Figure 6.

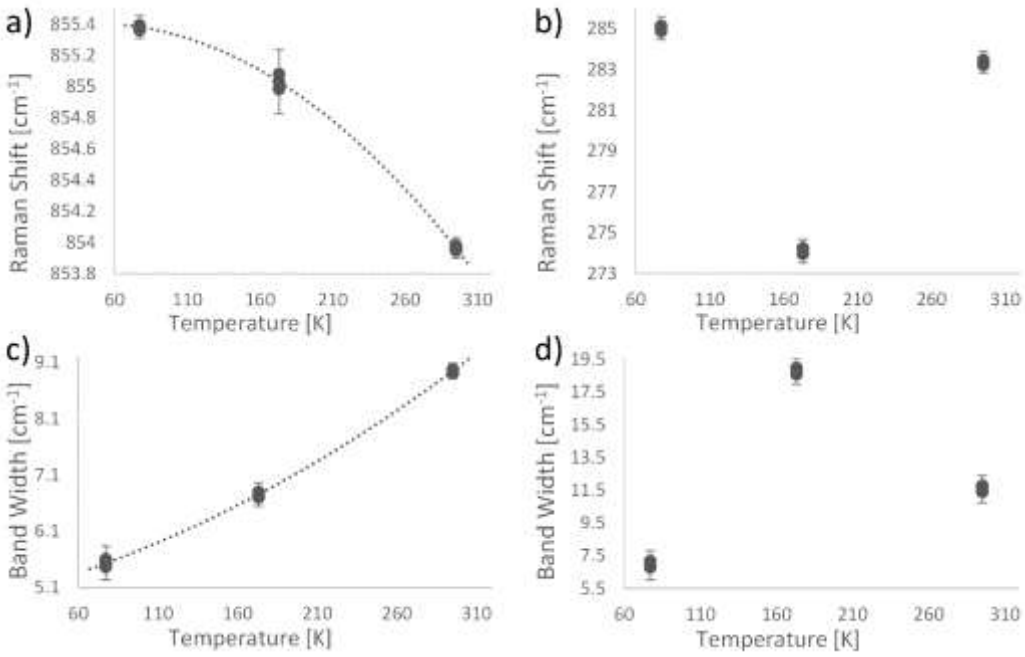

Figure 6 Alanine profile of Raman band shift and width change as a function of temperature for the C-CH_3 stretching band at 854 cm^{-1} (a and c) and NH_2 and CH_3 rocking band at 283 cm^{-1} (b and d). A general trend of the change, similar to Glycine Raman shift and width change profile, is highlighted in a and c. These bands are highlighted with arrows in the spectra in Figure 5. 3σ error bars

calculated for these peaks at each temperature over 3 measurements at 3 different power settings are included to indicate the relative significance of the changes.

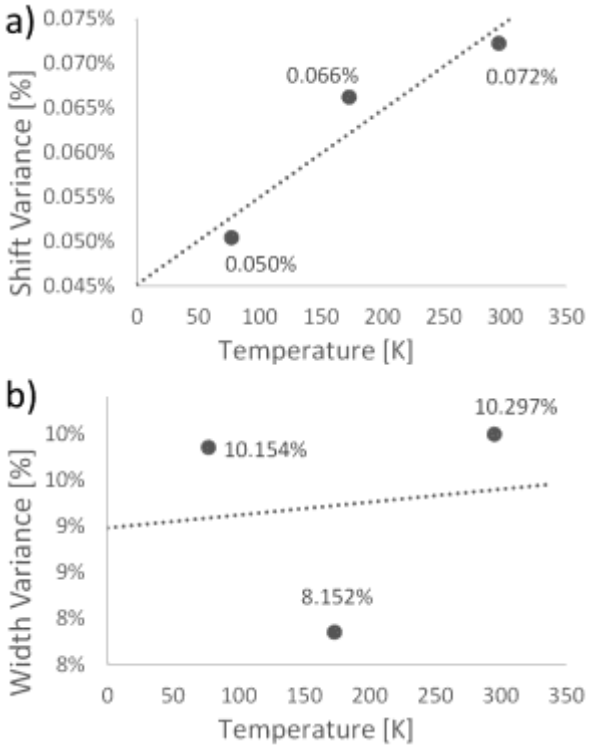

Figure 7 Variance of Raman band shift (a) and width (b) across individual Alanine spectra as a function of temperature

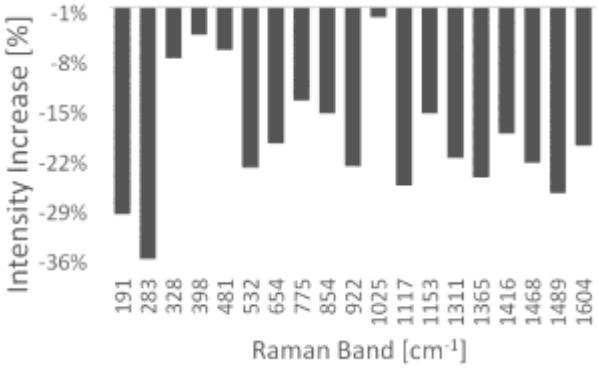

Figure 8 Intensity decrease of Alanine Raman spectra at 196 ^{O}C compared to room temperature measurements

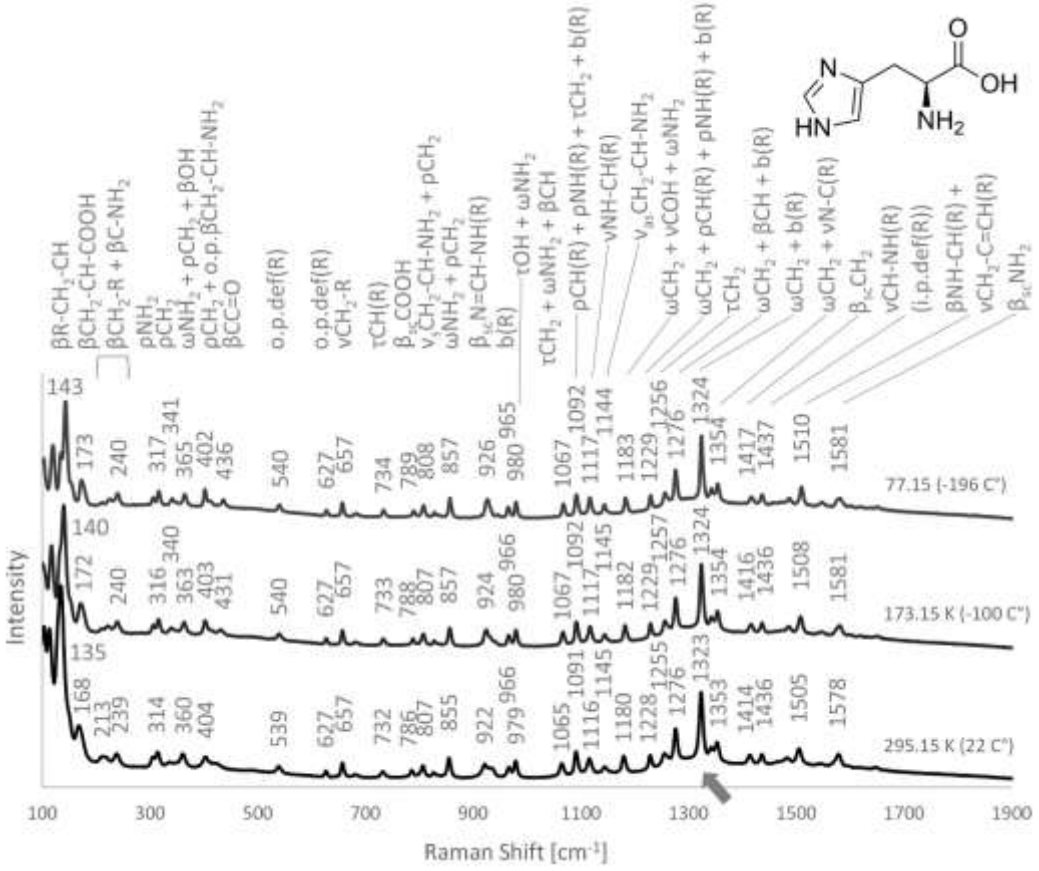

Figure 9 Raman spectra of Histidine at 22 ^{O}C, -100 ^{O}C and -196 ^{O}C, where R = ring (i.e. imidazole ring), ν = stretching, ω = wagging, ρ = rocking, β = bending, τ = torsion, b = breathing (i.e. in phase stretching of the ring), def = deformation (i.e. out of phase stretching of the ring), sc = scissoring, as = asymmetric, s = symmetric, o.p = out of plane, i.p. = in plane, brackets denote the location of the vibration. Assignments are based on an optimized DFT vibrational frequency calculation using SVP and polarizability calculations for Raman vibrational frequencies and Raman activity together with a review of previously published

assignments (Deckert-Gaudig & Deckert, 2009; Kumar et al., 2010; Martusevičius et al., 1996; Mesu et al., 2005; Zhu et al., 2011). A diagonal arrow highlights the band detailed in Figure 10.

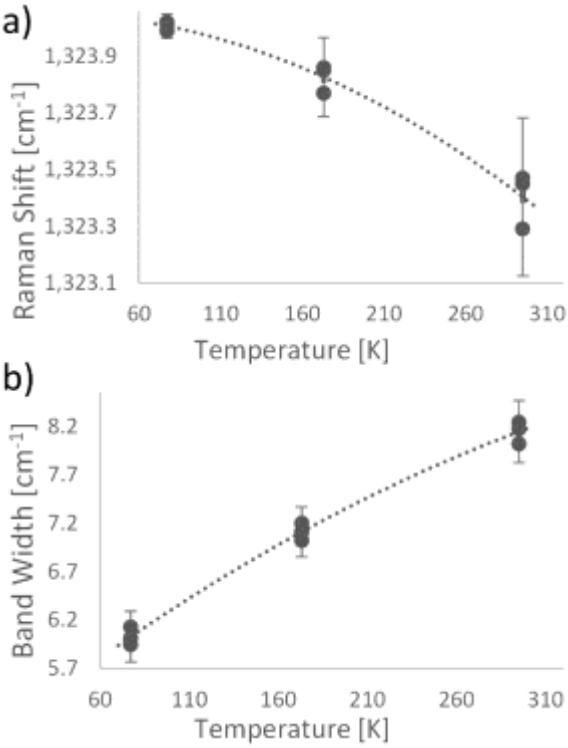

Figure 10 Histidine profile of Raman band shift and width change as a function of temperature for the 1323 cm^{-1} band (a and b respectively) assigned to mixed vibrations of CH_2 wagging and ring breathing. A general trend of the change is highlighted. This band is highlighted with an arrow in the spectra in Figure 9. 2σ error bars calculated for this Raman band at each temperature over 3

measurements at 3 different power settings are included to indicate the relative significance of the changes.

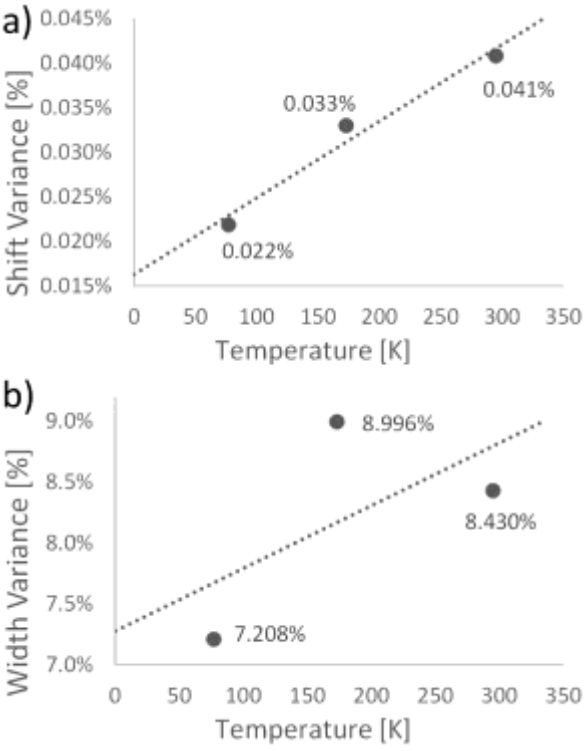

Figure 11 Variance of Raman band shift (a) and width (b) across individual Histidine spectra as a function of temperature

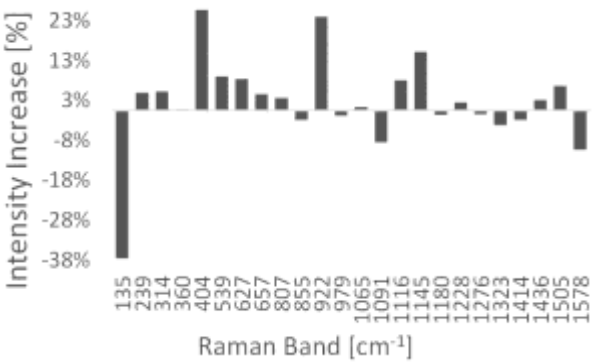

Figure 12 Intensity increase of Histidine Raman spectra at -196 ^{O}C compared to room temperature measurements

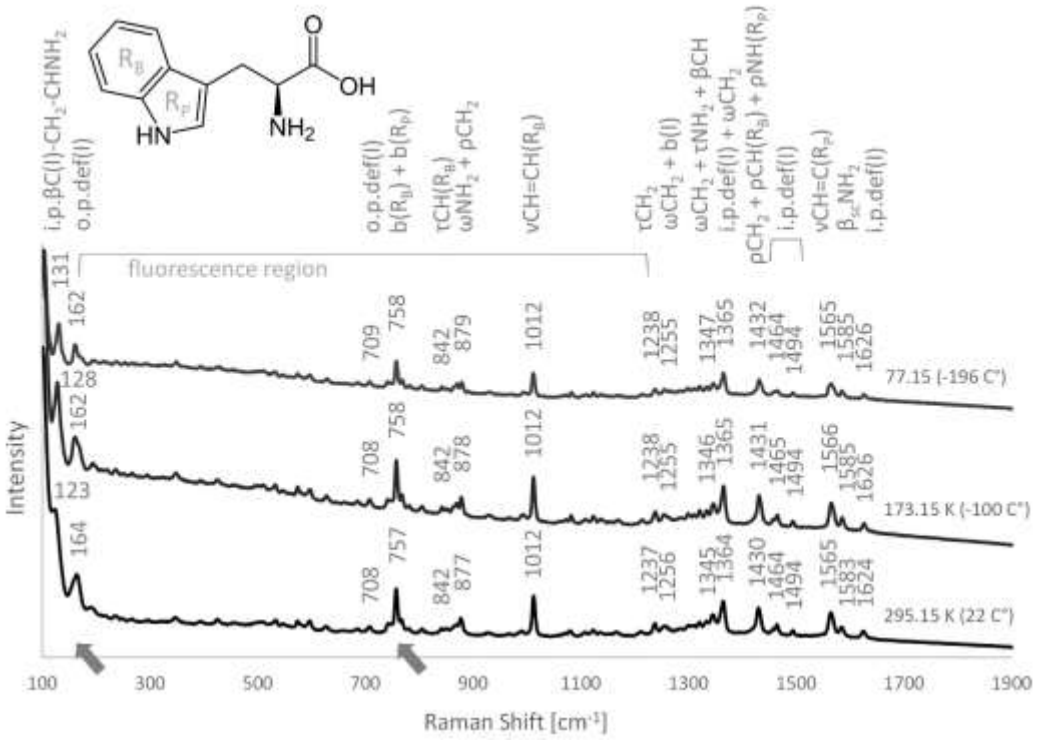

Figure 13 Raman spectra of Tryptophan at 22 ^{O}C, -100 ^{O}C and -196 ^{O}C, where R_B = benzene ring, R_P = pyrrole ring, I = indole group (i.e. benzene and pyrrole ring), ν = stretching, ω = wagging, ρ = rocking, β = bending, τ = torsion, b = breathing (i.e. in phase stretching of a ring), def = deformation (i.e. out of phase stretching of a ring), sc = scissoring, o.p = out of plane, i.p. = in plane, brackets denote the location of the vibration. Assignments are based on an optimized DFT vibrational frequency calculation using SVP and polarizability calculations for Raman vibrational frequencies and Raman activity together with a review of previously published assignments (Chuang & Chen, 2009; Freire et al., 2017). Diagonal arrows highlight the bands detailed in Figure 15.

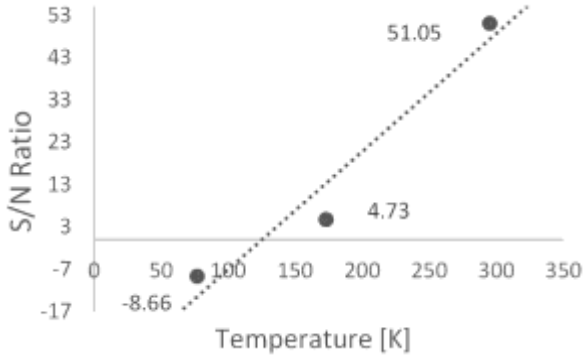

Figure 14 Average S/N ratio of Tryptophan fluorescence as a function of temperature

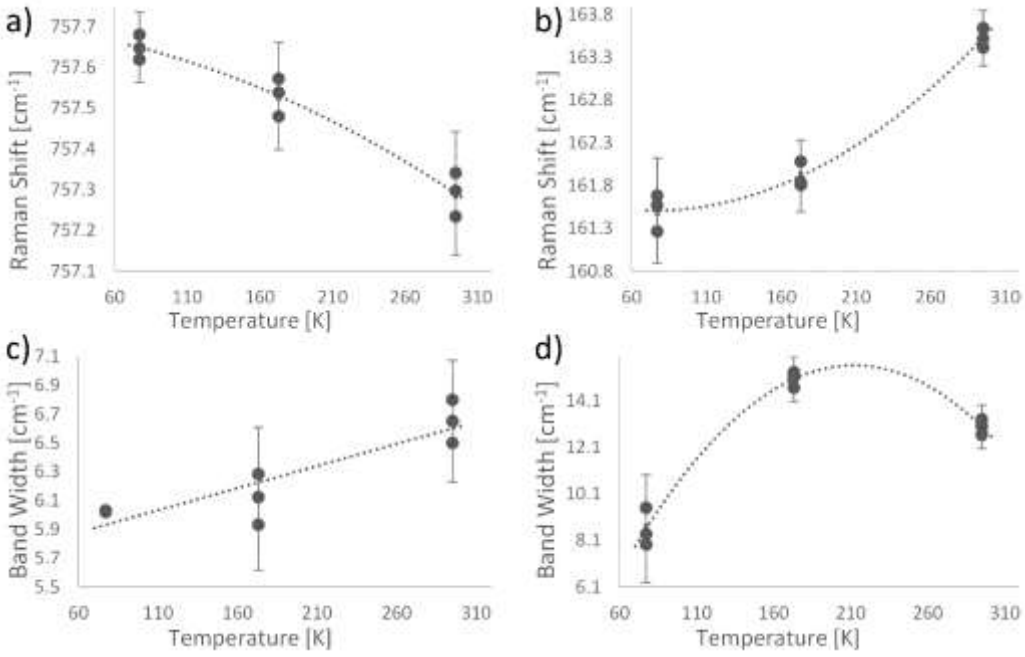

Figure 15 Tryptophan profile of Raman band shift and width change as a function of temperature for the benzene and pyrrole ring breathing band at 757 cm^{-1} (a and c) and the indole out of plane deformation band at 164 cm^{-1} (b and d). A general

trend of the change is highlighted. These bands are highlighted with arrows in the spectra in Figure 13. 2σ error bars calculated for these Raman bands at each temperature over 3 measurements at 3 different power settings are included to indicate the relative significance of the changes.

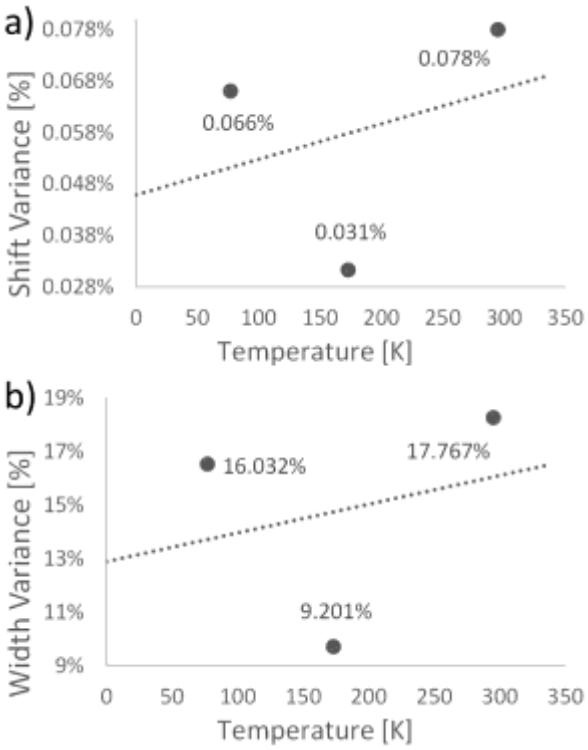

Figure 16 Variance of Raman band shift (a) and width (b) across individual Tryptophan spectra as a function of temperature

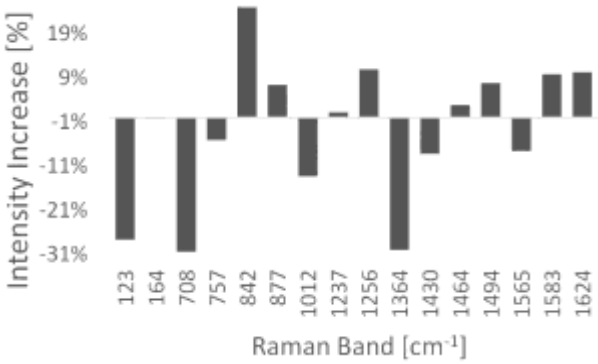

Figure 17 Intensity increase of Tryptophan Raman spectra at -196 ^{O}C compared to room temperature measurements

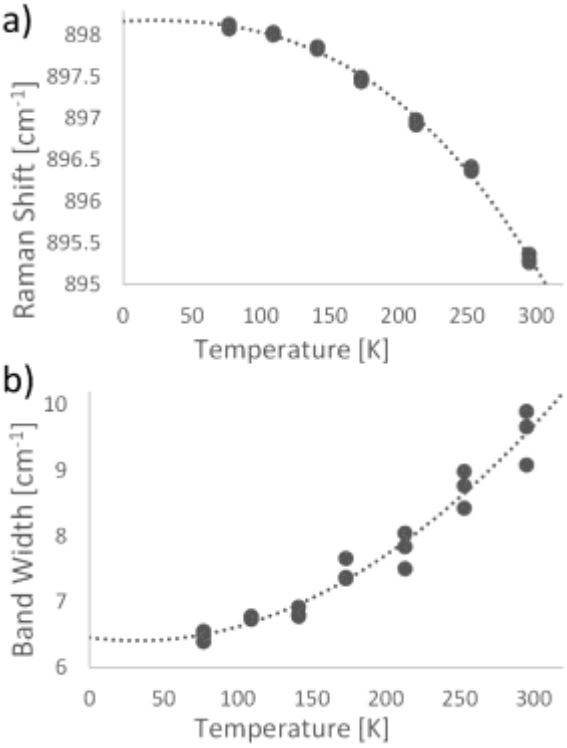

Figure 18 (a) The profile of the Raman shift change of Glycine band 895 cm^{-1} as a function of temperature and (b) the profile of the Raman band width change of Glycine 1331 cm^{-1} band as a function of temperature. A theoretical prediction corresponding to the general trend characterized by a 3rd order polynomial relationship for temperatures approaching 0 K is highlighted.

13. Tables

Band (Figure 1)	v1	v2	v3	v4	v5	v6	v7	v8	v9	v10	v11	v12	v13	v14	v15	v16	v17
Raman shift at 22 ^{O}C	163			358	497		602	699	895	1039	1112	1144	1331	1417	1446	1462	1576
new bands*		185 (-100 ^{O}C)	196 (-20 ^{O}C)			509 (-20 ^{O}C)											
Raman shift at -100 ^{O}C	168	185	204	361	491	516	604	702	897	1041	1118	1147	1332	1421	1447	1464	1579
Raman shift at -196 ^{O}C	171	188	208	363	492	522	605	703	898	1041	1120	1149	1332	1422	1447	1465	1580

Table 1 Glycine Raman bands at 22 ^{O}C, -100 ^{O}C and -196 ^{O}C (*temperature at which the new band is first detectable in the brackets)

Temperature [°C]		Glycine [cm^{-1}]	L-Alanine [cm^{-1}]	L-Histidine [cm^{-1}]	L-Tryptophan [cm^{-1}]
Minimum Band Clearance	22	15.99	21.09	12.43	18.75
	-100	17.06	21.53	13.91	17.41
	-196	16.76	22.35	14.75	16.60
Minimum Band Width	22	5.72	5.81	1.81	4.20
	-100	4.42	4.36	2.65	3.64
	-196	3.20	4.18	2.66	3.16

Table 2 Minimum clearance between adjacent Raman bands and Raman band width in the spectra of Glycine, Alanine, Histidine and Tryptophan at room temperature, -100 °C and -196 °C

Room Temperature								
Amino acid(s) in a mixture with Histidine	Clearance between bands [cm^{-1}]						Suggested minimum spectral resolution necessary [cm^{-1}]	Suggested ideal spectral resolution [cm^{-1}]
	12.43	10	7	5	4	2		
	Number of peaks							
Glycine	8	7	6	5	4	3	<4.23	<2.8
Alanine	12	9	7	6	6	6	<2.64	<1.51
Tryptophan	8	6	4	2	1	1	<7	<4.5
Glycine Alanine Tryptophan	19	17	13	11	10	10	<2	<1.51
-196 ^{O}C								
Amino acid(s) in a mixture with Histidine	Clearance between bands [cm^{-1}]						Suggested minimum spectral resolution necessary [cm^{-1}]	Suggested ideal spectral resolution [cm^{-1}]
	14.75	10	7	5	4	3		
	Number of peaks							
Glycine	8	7	6	4	4	4	<4	<2.74
Alanine	15	13	10	8	7	6	<2.02	<1.92
Tryptophan	7	6	5	3	1	1	<7	<5
Glycine Alanine Tryptophan	21	21	16	13	11	11	<2.02	<1.92

Table 3 The number of adjacent bands within potential mixtures of Glycine, Alanine, Histidine and Tryptophan with a suggested minimum spectral resolution necessary for full identification of these amino acids at room temperature and at -196 ^{O}C